Nuclear Engineering and Technology 53 (2021) 1–18

Contents lists available at ScienceDirect

Nuclear Engineering and Technology

journal homepage: www.elsevier.com/locate/net

Original Article

Analysis of VVER-1000 mock-up criticality experiments with nuclear data library ENDF/B-VIII.0 and Monte Carlo code MCS

Fathurrahman Setiawan, Matthieu Lemaire, Deokjung Lee*

Department of Nuclear Engineering, Ulsan National Institute of Science and Technology, 50, UNIST-gil, Ulsan, 44919, South Korea

ARTICLE INFO

Article history:
Received 26 February 2020
Received in revised form
3 June 2020
Accepted 10 June 2020
Available online 3 August 2020

Keywords:
MCS
Monte Carlo
VVER-1000 mock-up benchmark
LR-0 research reactor
Criticality analysis
Validation
ENDF/B-VIII.0

ABSTRACT

The criticality analysis of VVER-1000 mock-up benchmark experiments from the LR-0 research reactor operated by the Research Center Rez in the Czech Republic has been conducted with the MCS Monte Carlo code developed at the Computational Reactor Physics and Experiment laboratory of the Ulsan National Institute of Science and Technology. The main purpose of this work is to evaluate the newest ENDF/B-VIII.0 nuclear data library against the VVER-1000 mock-up integral experiments and to validate the criticality analysis capability of MCS for light water reactors with hexagonal fuel lattices. A preliminary code/code comparison between MCS and MCNP6 is first conducted to verify the suitability of MCS for the benchmark interpretation, then the validation against experimental data is performed with both ENDF/B-VII.1 and ENDF/B-VIII.0 libraries. The investigated experimental data comprises six experimental critical configurations and four experimental pin-by-pin power maps. The MCS and MCNP6 inputs used for the criticality analysis of the VVER-1000 mock-up are available as supplementary material of this article.

1. Introduction

This work presents a Monte Carlo interpretation with the nuclear data libraries ENDF/B-VII.1 and ENDF/B-VIII.0 of criticality experiments carried out in the VVER-1000 mock-up installed in the LR-0 research reactor operated by the Research Center Rez in the Czech Republic. The VVER-1000 mock-up is an integral experiment composed of a VVER hexagonal fuel lattice and of external elements that play the role of external VVER core components (such as the reactor pressure vessel - RPV). The mock-up is dedicated to the study of the neutron and photon physics parameters of VVER-type reactors. A specific purpose of the mock-up is the evaluation of the neutron fluence in the RPV through the measurements of neutron spectra in the external mock-up core components and the experimental determination of radial pin power maps for the pins in the outer region of the mock-up core that contribute the most to the neutron fluence in the RPV. The neutron fluence in the RPV is a highly important parameter for plant life management because it is responsible for the shift of the ductile-to-brittle transition temperature of the RPV [1]. The neutron fluence in the RPV limits the operating life of a plant since an RPV that becomes too brittle cannot be replaced after the plant started operation.

Experiments conducted in the VVER-1000 mock-up and available in the literature for code and nuclear data validation include the measurements of the neutron multiplication factor (k_{eff}) of the VVER-1000 mock-up for six critical configurations [2,3], measurements of relative radial power profiles and of neutron and photon spectra compiled inside the SINBAD database and known as “NEA-1517/82” [4], and several relative and absolute measurements of radial pin power maps [5–7]. This work focuses on the interpretation of the k_{eff} for the six critical configurations, and on the analysis of the four maps of measured radial pin powers. The criticality analysis is conducted with the Monte Carlo code MCS developed at the Ulsan National Institute of Science and Technology (UNIST), and is repeated with two different neutron data libraries, ENDF/B-VII.1 and ENDF/B-VIII.0.

The objectives of this work are multifold. First, a consistent interpretation of VVER-1000 mock-up criticality measurements presented in different sources across the literature is provided with one single mock-up model and one single Monte Carlo code. Second, the potential differences between the most up-to-date ENDF/B-VIII.0 library and its predecessor, the ENDF/B-VII.1 library, are

* Corresponding author. Department of Nuclear Engineering, Ulsan National Institute of Science and Technology, Bldg. 112, room 501-6, 50 UNIST-gil, Ulsan, 44919, South Korea.
E-mail addresses: setiawanfrs@unist.ac.kr (F. Setiawan), mlemaire@unist.ac.kr (M. Lemaire), deokjung@unist.ac.kr (D. Lee).

https://doi.org/10.1016/j.net.2020.06.015

assessed when those libraries are applied for the criticality simulation of the VVER-1000 mock-up. Third, this work aims at providing validation elements of the Monte Carlo code MCS for VVER criticality application, and a reference Monte Carlo solution for the future verification studies of the deterministic codes STREAM [8] and RAST-K 2.0 [9] also developed at UNIST. Fourth, the modelling work of the VVER-1000 mock-up performed in this work is made available to the community by sharing as supplementary material the MCS and MCNP6 inputs used during the interpretation. Finally, this work constitutes a first step towards the future shielding analysis of the VVER-1000 mock-up, i.e. the interpretation of the neutron and photon spectrum measurements from the VVER-1000 mock-up, since a good understanding of the criticality configurations and of the pin power distribution of the mock-up is required before tackling the shielding analysis.

A brief survey of the literature dealing with the interpretation of the VVER-1000 mock-up criticality experiments is presented. An interpretation of the k_{eff} values of the VVER-1000 mock-up for the six criticality configurations was conducted in Ref. [3] with the MCNPX code and seven nuclear data libraries: ENDF/B-VI.2, ENDF/B-VII.0, JEFF 3.1, JENDL 3.3, JENDL 4, ROSFOND 2009 and CENDL 3.1. The best agreement between calculation and experiments for the six critical configurations was observed with the CENDL 3.1 library with C-E (calculation minus experiment) discrepancies of about −65 pcm on average. The average C-E discrepancies amounted to about −433 pcm for the ENDF/B-VI.2 library and +236 pcm for the ENDF/B-VII.0 library. The technological uncertainty was evaluated by means of the direct perturbation method for six different parameters (boric acid concentration, moderator level, fuel enrichment, fuel density, fuel assembly pitch and clad thickness) and amounted in total to about 285 pcm at 3 standard deviations (average for the six critical cases).

Regarding previous interpretations of the four radial maps of measured pin powers from the VVER-1000 mock-up, the first radial map of 260 measured pin powers was presented and analyzed in the reference [4] with the 3-D diffusion code MOBY-DICK and the BUGLE-96 data suite based on ENDF/B-VI. The authors concluded that the MOBY-DICK calculations were to be “recommended as a neutron source” for the shielding analysis given the “modest” C/E (calculation over experiment) discrepancies between calculated and experimental pin powers. The second radial map of 52 measured pin power powers was presented and analyzed in Ref. [5] with MOBY-DICK/BUGLE-96, and with the MCNPX code and the seven libraries mentioned previously. The authors found “a satisfactory agreement between calculations and experiments in all regions non-adjacent to the reactor baffle. At the core and baffle boundary, C/E discrepancies were observed between experiments and MOBY-DICK whereas the C/E agreement was satisfactory for MCNPX but slightly worse than in different positions of the core”. The third radial map of 96 measured pin powers was presented and analyzed in Ref. [6] by the same authors with the same calculation tools. For the MCNPX calculations, a good agreement was observed with C/E agreement within 1 standard deviation (1σ) for 80% of the pins and at 3 standard deviations (3σ) for all the pins. The fourth and last radial map of 28 measured pin powers was presented and analyzed in Refs. [7] with MCNPX and the libraries ENDF/B-VII.0, JEFF 3.1 and JENDL 3.3. The authors found a satisfactory C/E agreement with 90% of the C/E results within 1σ. As a conclusion of this literature survey, to our best knowledge, the VVER-1000 mock-up experiments have not yet been interpreted with the most up-to-date library ENDF/B-VIII.0, and therefore this work will provide additional validation elements for ENDF/B-VIII.0 applied to VVER criticality analysis.

The plan of the paper is as follows. The geometry of the VVER-1000 mock-up and the calculation tools (MCS and nuclear data libraries) are presented in Section 2, and the investigated experimental data from the VVER-1000 mock-up is described in Section 3. Then, the modeling work of the mock-up for the MCS and MCNP6 codes and the calculation conditions are detailed in Section 4. Section 5 deals with the interpretation of the six critical configurations of the mock-up and includes an analysis of the sensitivity of the neutron multiplication factors to the technological parameters of the mock-up. Section 6 deals with the interpretation of the pin power measurements by means of the relative comparison of measured pin powers against calculated ones. All the pin power comparison results are analyzed with a statistical chi-square test to assess the behavior of the calculation/experiment (C/E) ratios. Both Sections 5 and 6 start with a preliminary verification of MCS versus the reference Monte Carlo code MCNP6 at equal nuclear data library (ENDF/B-VII.1) to establish the suitability of the MCS code for the interpretation of the VVER-1000 mock-up criticality experiments. Finally, Section 7 draws out the conclusions and research perspectives after this work.

2. Reactor geometry and calculation tools

2.1. VVER-1000 mock-up

The VVER-1000 mock-up is an integral benchmark experiment conducted in the LR-0 research reactor, a light-water-moderated zero-power reactor, operated by the Research Center Rez in the Czech Republic. The maximum continuous power of the reactor is 1 kW. The mock-up reproduces a sector of a typical VVER core. It consists of 32 dismountable fuel assemblies in a hexagonal lattice with 23.6 cm pitch and full-scale component simulators of baffle, barrel, displacer, pressure vessel and biological shielding as shown in Fig. 1.

The fuel pins of the mock-up are ~1.35 m long with upper and bottom ends made of zirconium alloy. The core active fuel length is 1.25 m, shorter than the commercial VVER-1000 fuel which uses 3.50 m length fissile column. 32 fuel assemblies are present in the core: 31 assemblies containing 312 fuel pins and 1 fuel assembly containing 282 fuel pins (the central assembly #27 with a dry experimental channel of diameter 6.8 cm cladded with 2.5 mm-thick steel). The fuel pins are arranged in a triangular lattice with a pitch of 12.75 mm. The fuel pellets with ^{235}U enrichment of 2.0%, 3.0%, or 3.3% (respectively the yellow, orange and red assemblies in Fig. 1) are placed inside cladding tubes made of zirconium alloy. Along with fuel pins, each assembly contains 18 absorber cluster tubes made of stainless steel and a central zirconium-alloy tube. Natural boron carbide is used as neutron-absorber elements. Five 2-cm-high spacer grids are attached on each fuel assembly with the grid centers located 24.4, 49.9, 75.4, 100.9, and 126.4 cm from the bottom of the active core. A displacer gap filled with air is placed between the barrel simulator and the LR-0 tank to simulate the water density reduction that occurs during the operation of commercial VVER-1000 reactors.

Two cluster tube lattice configurations are employed in the mock-up core as shown in Fig. 2. The configuration on the right-hand side corresponds to the configuration employed in commercial VVER-1000 reactors. In the VVER-1000 mock-up, it is only used for the two assemblies with 3.3% fuel enrichment (assemblies #9 and #17) whereas the configuration on the left-hand side is used for all the other assemblies. Fig. 2 also presents the numbering of the pins for the two kinds of assemblies used in the VVER-1000 mock-up. For convenience, pin locations are referred in future tables as XX_YY where XX is the fuel assembly number and YY is the pin number inside the assembly.

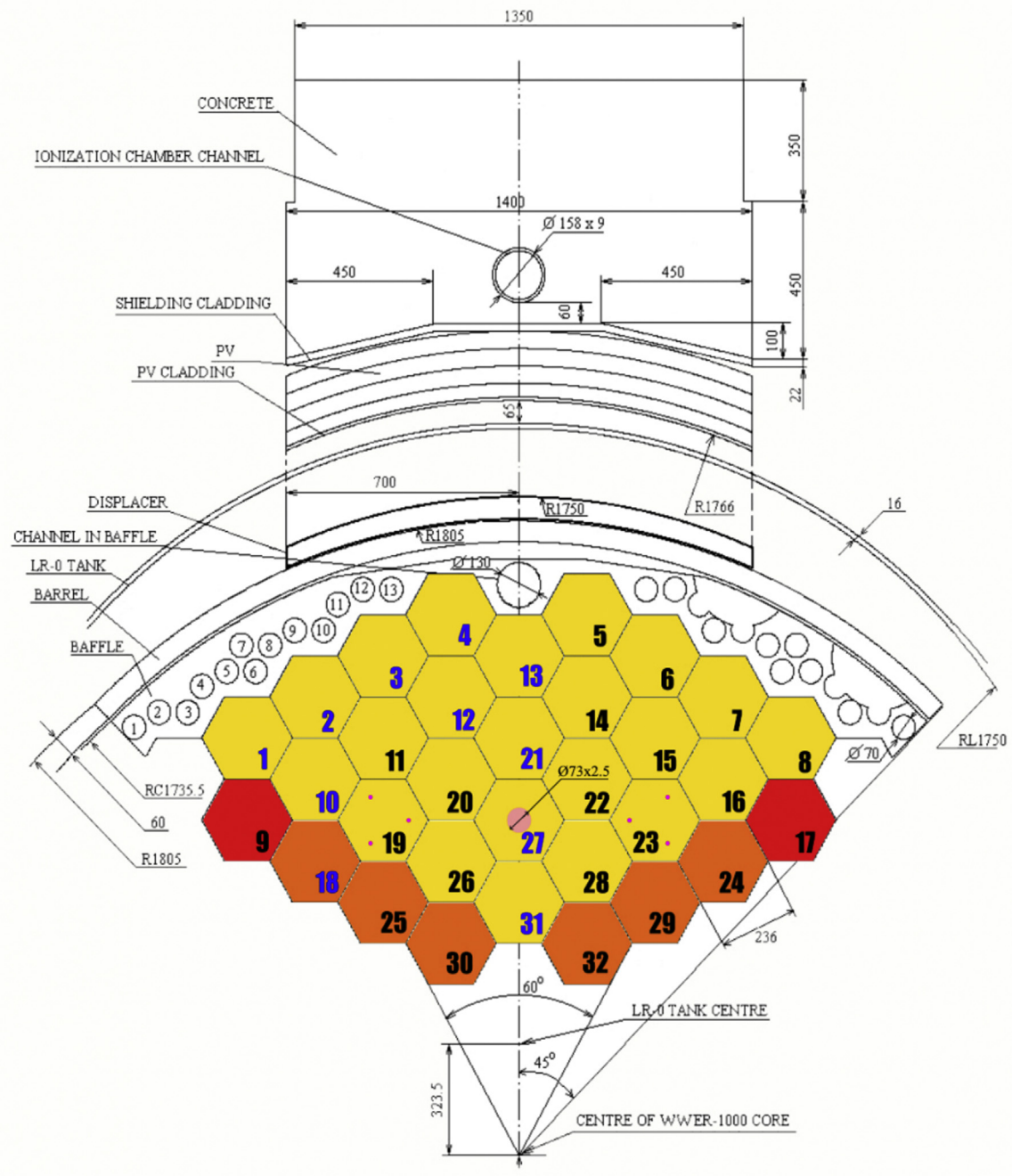

Fig. 1. VVER-1000 mock-up arrangement inside the LR-0 reactor [4]. Blue numbers depict the assemblies with available measured pin powers. (For interpretation of the references to color in this figure legend, the reader is referred to the Web version of this article.)

2.2. MCS Monte Carlo code

MCS [10,11] is a neutron-photon transport code based on the Monte Carlo method and developed at the Computational Reactor Physics and Experiment (CORE) laboratory of the Ulsan National Institute of Science and Technology (UNIST) for the main purpose of whole-core calculation with high-fidelity and high-performance. Geometry modelling in MCS is based on constructive solid geometry (CSG) and reactors with square and hexagonal fuel lattices can be modelled in MCS. Validation of MCS neutron transport capability for square fuel lattices has notably been performed against ~300 selected ICSBEP critical benchmarks (International Criticality Safety Benchmark Evaluation Project) [12] and against the BEAVRS benchmark (Benchmark for Evaluation and Validation of Reactor Simulations) [13]. Verification of MCS neutron transport capability for hexagonal fuel lattice includes criticality calculations for the China Experimental Fast Reactor (CEFR) [14].

2.3. ENDF/B-VII.1 and ENDF/B-VIII.0 nuclear data libraries

The VVER-1000 mock-up criticality calculations are conducted with two successive versions of the nuclear data library ENDF/B released by the Cross Section Evaluation Working Group (CSEWG), namely ENDF/B-VII.1 [15], released in 2011, and the most recent ENDF/B-VIII.0 [16], released in 2018 with updated evaluations of important nuclides that impact nuclear criticality simulations. The

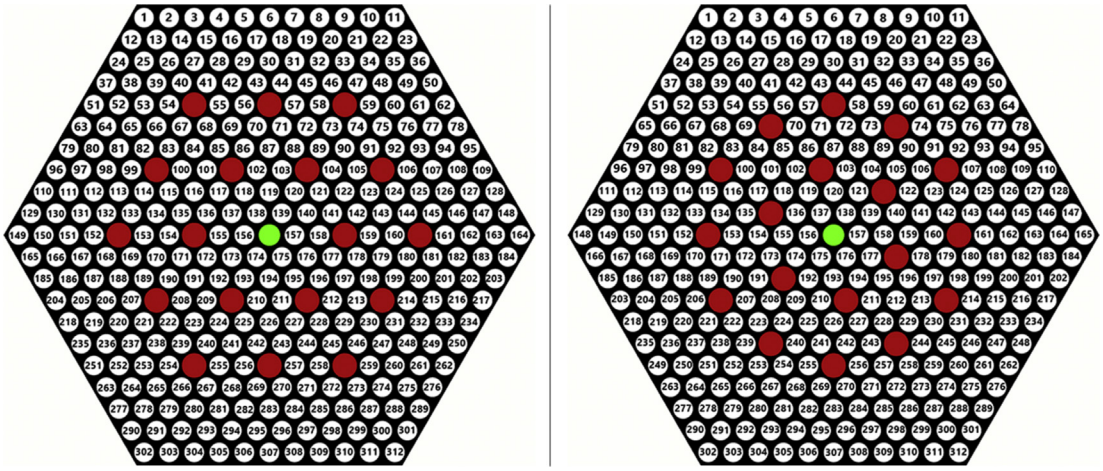

Fig. 2. The two cluster tube configurations used in VVER-1000 mock-up assemblies.

changes between the two libraries for the materials present in the VVER-1000 mock-up that can have an impact on the criticality analysis of the VVER-1000 mock-up experiments are shortly described:

- ^{1}H (water moderator): updated (n,elastic) cross section.
- ^{10}B (boric acid in the moderator): updated (n,α) cross section.
- $^{54,56-58}$Fe (steel structural materials): updated neutron cross sections.
- $^{58-62,64}$Ni (steel structural materials): updated neutron cross sections.
- ^{235,238}U: updated neutron cross sections, updated prompt fission neutron spectrum and updated prompt neutron multiplicity ($\bar{\nu}$).
- ^{239}Pu: updated neutron cross sections, updated prompt fission neutron spectrum and updated prompt neutron multiplicity ($\bar{\nu}$).

3. Experimental data from the VVER-1000 mock-up

This section provides a short description of the investigated criticality experiments. Two kinds of measurement data are analyzed: the effective neutron multiplication factors (k_{eff}) from six critical VVER-1000 mock-up configurations and the radial pin powers from four distinct measurement campaigns in the VVER-1000 mock-up. The six different critical configurations were achieved by adjusting the moderator level, boric acid concentration and absorber rod positions. For convenience purpose, the experiments dealing with pin power measurements are summarized in Table 1 and they will be denoted throughout this paper after the specific names listed in Table 1.

3.1. Critical configurations of VVER-1000 mock-up

The VVER-1000 mock-up criticality experiments were carried out at room temperature and pressure with continuous maximal power of 1 kW. The experiments were organized with different critical configurations by varying the moderator level (reported from the bottom of the active core) and boric acid concentration as listed in Table 2 [5]. The cases 1 to 5 are in all-rod-out condition whereas six absorber rods are partially inserted in assemblies #19 and #23 in case 6. The critical configuration for the 4 distinct measurements of pin powers corresponds to the sixth critical configuration (case 6).

3.2. SINBAD-1 experiment

A short review of the information from the reference [4] is presented. The VVER-1000 mock-up benchmark data compiled in the SINBAD database consists of the measurements of relative pin powers for 260 pins mainly located in the peripheral region of the mock-up core as shown in Fig. 3. The core power during the measurements is not indicated in the documentation. The relative pin power was measured by means of post-irradiation gamma scanning of fuel pins in the 5-cm region on the central mid-plane of the mock-up core. No information is given about the measured fission products, the duration of the fuel irradiation and the cooling time between the end of the fuel irradiation and the measurements of the gamma activities of the fission products. The measured data of relative pin powers for the 260 pins is given normalized so that the mean value for the 260 pins equals 1000. The experimental uncertainties are available for each measured pin and range from 2.0% (1σ) to 5.0% (1σ) with a root-mean-square (RMS) uncertainty of 3.3% (1σ). The structure of the experimental uncertainties is not described, only a total value of experimental uncertainty is given.

3.3. BENCHMARK-2 experiment

A short review of the information from the reference [5] is presented. The fission rates of 52 pins from 7 different assemblies of the VVER-1000 mock-up were measured by means of post-

Table 1
List of analyzed pin power measurements from the VVER-1000 mock-up.

Experiment name	Measurements characteristic	Number of measured pins	Measured assemblies	References
SINBAD-1	Relative	260	#3, #4, #12, #13, #21, #27, #31	[4]
BENCHMARK-2	Relative	52	#3, #4, #12, #13, #21, #27, #31	[5]
BENCHMARK-3	Absolute	96	#1, #2, #3, #10, #18	[6]
BENCHMARK-4	Absolute	28	#2	[7]

Table 2
VVER-1000 mock-up critical configurations with various moderator level and boric acid concentration.

Parameters	Case 1	Case 2	Case 3	Case 4	Case 5	Case 6
Moderator level [cm]	51.34	65.91	79.11	96.71	103.37	150.0
H_3BO_3 concentration [g/kg]	2.85	3.63	4.06	4.44	4.53	4.68
Control rod position	ARO[b]	ARO[b]	ARO[b]	ARO[b]	ARO[b]	6 rods inserted[a]

[a] 64.6 cm inserted from top of active core.
[b] ARO: all rods out

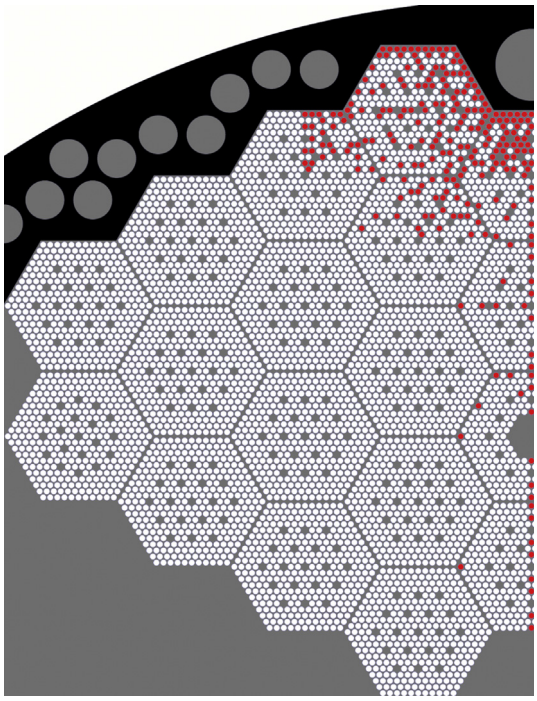

Fig. 3. Positions (in red) of the 260 pins measured in the SINBAD-1 experiment. (For interpretation of the references to color in this figure legend, the reader is referred to the Web version of this article.)

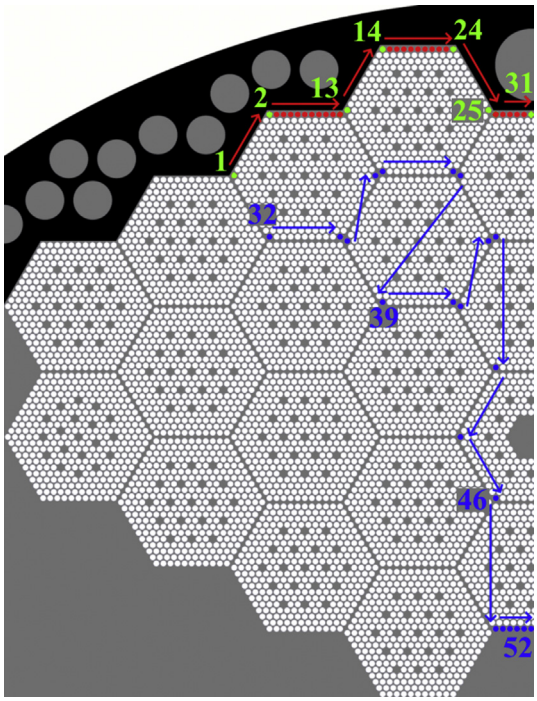

Fig. 4. Position of the 52 measured pins with their numbering sequence for the BENCHMARK-2 experiment.

irradiation gamma scanning of irradiated fuel. The reactor power during the fuel irradiation is not indicated in the reference. The positions of the 52 measured pins are shown in Fig. 4. The measurements were performed in the central 2-cm region of the fuel pins. The gamma spectra of the pair mother-daughter nuclei ^{140}Ba (half-life 12.75 days) and ^{140}La (half-life 1.68 days) were analyzed by means of gamma-ray spectroscopy with a HpGe detector and a multichannel analyzer. The pulse rates (net peak areas) were evaluated from the energy peaks 537 keV from ^{140}Ba and 1596 keV from ^{140}La. The measurements were performed 15 days after fuel irradiation to establish the transient equilibrium state between ^{140}Ba/^{140}La and apply a decay correction on both nuclides using the decay half-life of ^{140}Ba. The pulse rates for the 1596 keV energy peak were chosen to yield the relative pin power distribution according to a study showing that the fission product distribution can be considered proportional to the pin power distribution for the case of the VVER-1000 mock-up and the selected mother-daughter nuclei ^{140}Ba and ^{140}La. The relative powers of the 52 pins are given in arbitrary units (mean value of the 52 relative powers $\simeq$ 2455).

The experimental uncertainties are dominated by the uncertainties from the determination of the pulse rates (gross peak area, Compton continuum area, background area, parameters in the energy and peak shape calibration). The reference only reports the "total C/E−1 uncertainty", which range from 2.2% to 10.5%. We consider those values to be the quadratic sum of calculation and experimental uncertainties and they are assumed at 1 standard deviations. To retrieve the experimental uncertainties, we assume a flat calculation uncertainty of 1.7% for all the pins based on reference [6]. Therefore, the experimental uncertainties adopted for the criticality interpretation range from 1.4% (1σ) to 10.4% (1σ) with an RMS value of about 5.7% (1σ).

3.4. BENCHMARK-3 experiment

A short review of the information from the reference [6] is presented. The determination of the absolute pin power of 96 pins was conducted by means of ^{92}Sr fission product activity measurements. The positions of the 96 pins are indicated in Fig. 5. The fuel was irradiated with 5 batches of 2.5 h each at a reactor power of about ~10 W. The gamma-scanning measurements were performed at the 5-cm central region of each fuel pin with HpGe spectrometry at short time (about 30 min) after reactor shutdown. The pulse rates (net peak areas) of the energy peak at 1384 keV of ^{92}Sr were measured. Decay corrections were calculated due to the short half-life of ^{92}Sr (2.6 h) with regards to the cooling time between reactor shutdown and measurements. The measured pulse rates of each batch were normalized to the reaction rate during the first irradiation batch (power = 9.5 W). The absolute reactor power was determined by the neutron flux method (using the ^{197}Au (n,γ) reaction) and independent power monitoring by a compensated boron chamber.

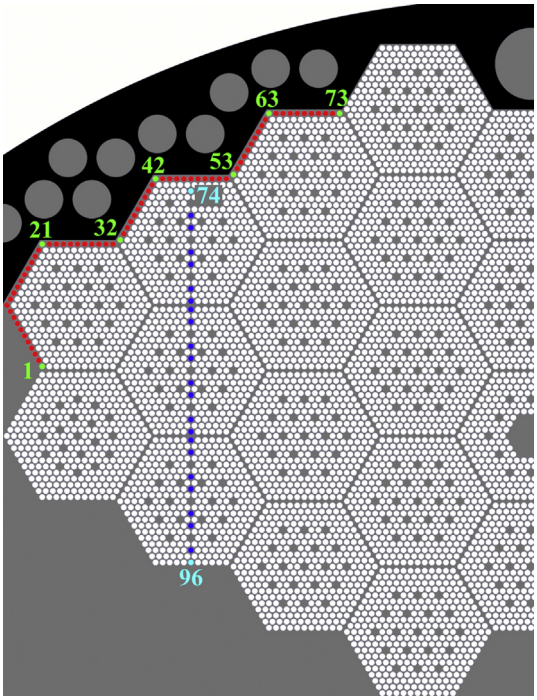

Fig. 5. Position of the 96 measured pins with their numbering sequence for the BENCHMARK-3 experiment.

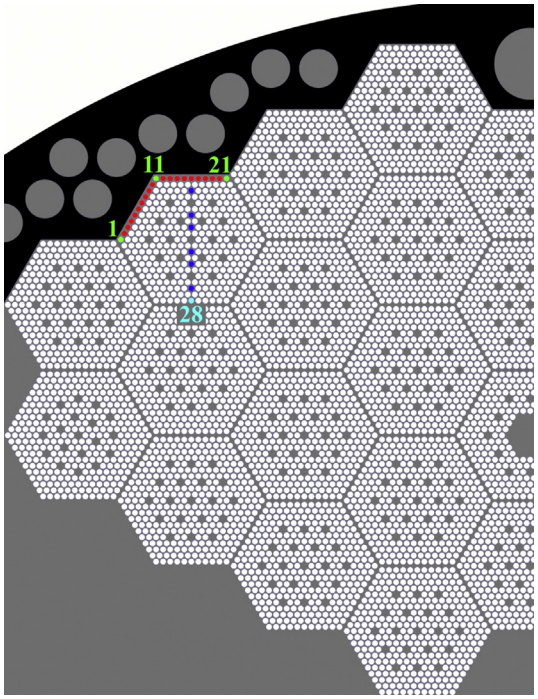

Fig. 6. Position of the 28 measured pins with their numbering sequence for the BENCHMARK-4 experiment.

The experimental data consists in the absolute net peak areas for each fuel pin. For each pin, the total C/E−1 uncertainty is provided and range from 3.6% (1σ) to 4.2% (1σ), with a statistical calculation uncertainty below 1.7% (1σ). The main sources of experimental uncertainties are presented at 1 standard deviation and include the following uncorrelated components: pulse rate counting (about 1.5%), fission product yields (about 1.5%), activation foil measurements (below 2.5%), activation foil position (about 1%), and boric acid concentration (below 0.9%). For the MCS criticality interpretation, only a relative C/E comparison of pin powers is performed and only the experimental uncertainties linked to pulse rate counting and boric acid concentration are therefore retained. For each pin, the resulting total experimental uncertainty for the purpose of relative C/E comparison ranges from 1.7% (1σ) to 2.7% (1σ).

3.5. BENCHMARK-4 experiment

A short review of the information from the reference [7] is presented. The determination of the absolute pin power of 28 pins located in the assembly #2 (see Fig. 6) was conducted by means of the measurements of the activity of five different fission products with specific energy peak: ^{140}Ba (537.3 keV), ^{103}Ru (497.1 keV), ^{131}I (364.5 keV), ^{141}Ce (145.4 keV) and ^{95}Zr (724.2 keV). The five selected fission products have the common feature of having much longer half-lives than their respective mother nuclides. The 28 pins selected for measurements are a subset of the 96 pins measured in BENCHMARK-2. After a VVER-1000 mock-up irradiation of 100 h at an average power of 630 W, the measurements of the fission products pulse rates (net peak areas) were realized after at least 16 days of cooling period (depending on the fission product) by means of HpGe spectroscopy on the 5-cm central region of the 28 fuel pins. The power of the reactor during the irradiation was monitored with independent measurements from a boron chamber and the absolute reactor power was determined by means of activation foil measurements.

The experimental data consists in the absolute net peak areas for each of the 28 pins and each of the 5 measured fission products. For each net peak area, the total C/E−1 uncertainty is provided and ranges from 1.5% (1σ) to 2.9% (1σ). The main experimental uncertainties are presented at 1σ and include the following uncorrelated components: uncertainty on the count rates (about 0.5%–1.5%), uncertainty on fission yields (1%–1.5%) and uncertainty on the boric acid concentration (lower than 0.8%). The uncertainties related to the determination of the absolute power of the reactor are not provided. For the purpose of relative C/E comparison, the fission yield uncertainties (assumed to equal 1.0%) and the calculation uncertainties (assumed to equal 1.7%) are quadratically subtracted from the total C/E−1 uncertainties and the total experimental uncertainties adopted for the relative C/E comparison range from 1.2% to 2.8% at 1σ.

4. Modelling of the VVER-1000 mock-up with MCS

There are at least two sources in the literature that extensively detail the geometry and material compositions of the VVER-1000 mock-up and that can be used to develop a model: the first one is available in the SINBAD benchmark documentation [4] and the other one is available in the IRPhE benchmark documentation [2]. The information present in those two sources sometimes contradict each other, especially regarding the fuel enrichment, fuel density and cladding thickness. For the purpose of criticality analysis with the MCS Monte Carlo code, the choice was made to develop a 3D model of the VVER-1000 mock-up core primarily based on the information of the IRPhE documentation.

The developed model includes the mock-up core (32 fuel assemblies), the external core components (baffle, barrel, and displacer), the core lower support structures (benchmark plate, standard support plate and bottom moderator reflector), and the shielding components. The information for the shielding components (reactor pressure vessel and biological shielding) is adopted

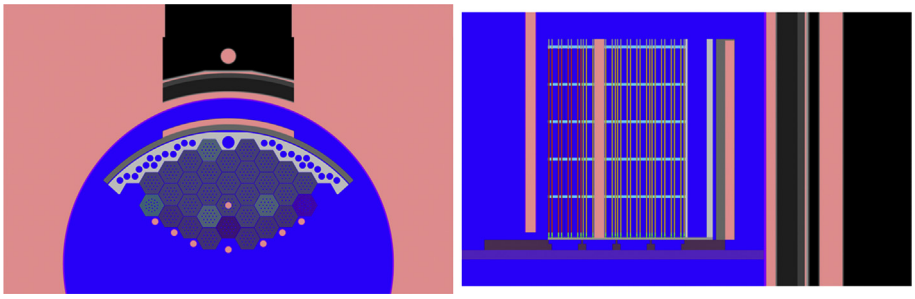

Fig. 7. MCS model of the VVER-1000 mock-up: XY-plane view (left) and YZ-plane view (right).

from the SINBAD documentation and modelled to complete the full VVER-1000 mock-up as shown in Fig. 7. The steel spacer grids of the assemblies are not modelled heterogeneously due to the complex honeycomb structure of the hexagonal fuel assemblies; they are modelled instead by means of band dissolution technique [17] where the water moderator and the steel spacer grids are homogenized at the level of the spacer grids only. The materials are modelled at atmospheric pressure and room temperature with regards to the experimental conditions. The axial views (YZ-plane plots generated with MCS) of the six critical configurations of the VVER-1000 mock-up models with moderator levels and boric acid concentrations as specified in Table 2 can be seen in Fig. 8.

In parallel with the MCS models, identical MCNP6 models of the VVER-1000 mock-up are written for comparison purpose. Identical ACE files (continuous energy neutron cross section and thermal scattering data) corresponding to the ENDF/B-VII.1 nuclear data library are used in MCS and MCNP6 for the comparison.

The MCS calculations of the six critical configurations and of the radial pin power map for experimental validation are conducted with the ENDF/B-VII.1 and ENDF/B-VIII.0 nuclear data libraries. The thermal scattering data S(α,β) for hydrogen in moderator from the appropriate nuclear data library (either ENDF/B-VII.1 or B-VIII.0) is used for all the calculations. For the six critical calculations, each simulation is carried out with 100 inactive cycles, 300 active cycles and 5×10^5 neutron histories per cycle. For the pin power calculation, 100 inactive cycles, 1000 active cycles and 10^6 neutron histories per cycle are employed. The stationarity of the fission source distribution after 100 inactive cycles is checked by means of the cell-wise Shannon entropy and the center of mass of the fission source distribution [18].

5. Analysis of six critical configurations of the VVER-1000 mock-up

5.1. Effective multiplication factors

The comparisons of effective neutron multiplication factors (k_{eff}) for the six critical configurations between MCS, MCNP6 and the experiments (k_{eff} equals unity) are presented in Table 3 for the ENDF/B-VII.1 library. Excellent agreement is observed between the two codes with a maximum difference of 14 ± 25 pcm (3σ). A consistent overprediction of the k_{eff} values in the range from +137 to +532 pcm is observed for the six cases. This overprediction remains for the comparison of k_{eff} values between MCS with the ENDF/B-VIII.0 library and the experimental k_{eff} values (= unity) shown in Table 4. The k_{eff} values calculated with ENDF/B-VIII.0 are not significantly different from the k_{eff} values calculated with ENDF/B-VII.1, with a maximum k_{eff} difference of only 27 ± 25 pcm between the two libraries.

The causes of k_{eff} discrepancies between calculations and experiments are most often multiple and can be rooted in the nuclear data and/or in geometrical and material composition discrepancies between the reactor and its calculation model. The next subsection is dedicated to the sensitivity analysis of the k_{eff} calculations to the geometrical and material composition parameters of the reactor so as to quantify the technological uncertainty on the calculated k_{eff} values.

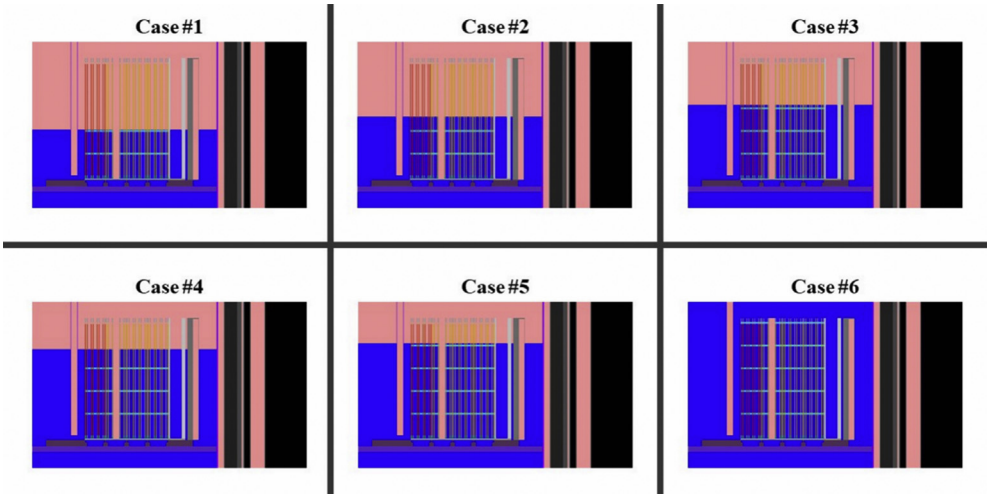

Fig. 8. Axial view (YZ-plane) of the six critical configurations of the VVER-1000 mock-up.

Table 3
ENDF/B-VII.1 library: comparison of k_{eff} values between MCS, MCNP6 and experiment ($k_{eff} = 1$).

Case	MCS ± 3σ	MCNP6 ± 3σ	(MCS − MCNP6) ±3σ [pcm]	MCS − EXP [pcm]
Case 1	1.00137 ± 18E-05	1.00132 ± 15E-05	5 ± 23	137
Case 2	1.00307 ± 18E-05	1.00309 ± 15E-05	−2 ± 23	307
Case 3	1.00403 ± 18E-05	1.00417 ± 18E-05	−14 ± 25	403
Case 4	1.00462 ± 15E-05	1.00468 ± 15E-05	−6 ± 21	462
Case 5	1.00495 ± 18E-05	1.00498 ± 15E-05	−3 ± 23	495
Case 6	1.00532 ± 18E-05	1.00523 ± 15E-05	9 ± 23	532

Table 4
ENDF/B-VIII.0 library: comparison of k_{eff} values between MCS and experiment ($k_{eff} = 1$).

Case	MCS ± 3σ	MCS − EXP [pcm]
Case 1	1.00153 ± 18E-05	153
Case 2	1.00321 ± 18E-05	321
Case 3	1.00429 ± 18E-05	429
Case 4	1.00483 ± 18E-05	483
Case 5	1.00523 ± 15E-05	523
Case 6	1.00559 ± 18E-05	559

Table 5
The reference (ref.) and perturbated (pert.) values of boric acid concentration, assembly pitch, and cladding thickness for sensitivity analysis.

Case	Boric acid (g/kg)		FA pitch (cm)		Clad-thick (cm)	
	Ref.	Pert.	Ref.	Pert.	Ref.	Pert.
Case 1	2.85	2.91	23.6	23.8	0.071	0.0726
Case 2	3.63	3.68	23.6	23.8	0.071	0.0726
Case 3	4.06	4.11	23.6	23.8	0.071	0.0726
Case 4	4.44	4.49	23.6	23.8	0.071	0.0726
Case 5	4.53	4.58	23.6	23.8	0.071	0.0726
Case 6	4.68	4.76	23.6	23.8	0.071	0.0726

Table 6
The reference (ref.) and perturbated (pert.) values of enrichment for sensitivity analysis.

Case	Enrichment	
Case 1-	Reference	Perturbated
Case 6	2.00%	1.99%
	2.01%	2.00%
	2.02%	2.01%
	3.01%	3.00%
	3.29%	3.28%
	3.30%	3.29%

Table 7
ENDF/B-VII.1 sensitivity analysis of k_{eff} to the technological parameters of the VVER-1000 mock-up.

Case	k_{eff}	Modelling Uncertainties (pcm) ± 3σ − ENDF/B-VII.1				
		Total	Boric acid	Enrichment	FA pitch	Clad-thick
Case 1	1.00137	300 ± 49	159 ± 23	146 ± 25	203 ± 25	46 ± 23
Case 2	1.00307	370 ± 51	151 ± 25	162 ± 25	294 ± 25	35 ± 25
Case 3	1.00403	376 ± 51	128 ± 25	146 ± 25	322 ± 25	10 ± 25
Case 4	1.00462	410 ± 42	135 ± 21	161 ± 21	352 ± 21	5 ± 21
Case 5	1.00495	416 ± 50	132 ± 25	146 ± 25	366 ± 25	6 ± 23
Case 6	1.00532	451 ± 49	209 ± 23	158 ± 25	367 ± 23	11 ± 25

5.2. Sensitivity to the modelling uncertainties

The sensitivity of the k_{eff} value to several parameters of the VVER-1000 mock-up are studied in this subsection. A previous sensitivity analysis [3] showed that the sensitivity of the k_{eff} to the uncertainties in the moderator level was negligible compared to the sensitivities to the boric acid concentration, the fuel assembly (FA) pitch, the cladding thickness, and the fuel enrichment. For this previous study, the statistical uncertainties associated with the Monte Carlo calculations amounted to 40–50 pcm at 3σ for both the perturbated and reference cases. Therefore, only the sensitivity of the k_{eff} to the four main parameters is studied below, with the objective to obtain smaller statistical uncertainties than before.

The sensitivity calculations are conducted separately with the ENDF/B-VII.1 and ENDF/B-VIII.0 nuclear data libraries. For each parameter, a calculation of the perturbated model C_{PERT} is conducted with MCS and compared against the MCS calculation of the reference model C_{REF} (direct perturbation method). The values of the perturbations for each parameter are taken from the IRPhE documentation [2]. The reference and perturbated values at 3σ for each parameter, are summed up in Table 5 and Table 6. The perturbated values are chosen so that the impact on the reactivity is negative (the perturbations decrease the k_{eff} values).

The individual technological uncertainty, defined as ($C_{PERT} - C_{REF}$) for each parameter, are shown in Table 7 for the ENDF/B-VII.1 library and Table 8 for the ENDF/B-VIII.0 library. The statistical uncertainties for each (C_{REF} - C_{PERT}) value are presented at 3σ. The total technological uncertainty and its statistical uncertainty are calculated as the quadratic sum of the individual uncertainties because the individual perturbations are uncorrelated.

With regards to the statistical uncertainty associated with the ($C_{PERT} - C_{REF}$) values, no significant difference is observed between the sensitivity analysis conducted with the ENDF/B-VII.1 and ENDF/B-VIII.0 libraries. Most of the total technological uncertainty comes from the uncertainties in the boric acid concentration, fuel enrichment and assembly pitch. The technological uncertainty due to the fuel assembly pitch increases strongly with the moderator level from case 1 to case 6, causing a global increase of the total technological uncertainty as well.

The (C-E) k_{eff} discrepancies with their uncertainties (from technological and statistical origins) are listed in Table 9. Other sources of uncertainties should be investigated in the future to advance further the criticality analysis, such as the propagation of the nuclear data uncertainties on the k_{eff} of the VVER-1000 mock-up and the impact of modelling heterogeneous spacer grids instead of band-dissolution spacer grids.

6. Analysis of the VVER-1000 mock-up radial and axial power distributions

Verification and validation (V&V) of the radial power distribution and axial distribution is performed in this section. The verification studies include the comparison of pin-by-pin power between MCS and MCNP6 and of axial power distribution between MCS, MCNP6 and a reference calculation from the diffusion code MOBY-DICK. The ENDF/B-VII.1 nuclear data library is employed for

Table 8
ENDF/B-VIII.0 sensitivity analysis of k_{eff} to the technological parameters of the VVER-1000.

Case	k_{eff}	Modelling Uncertainties (pcm) ± 3σ − ENDF/B-VIII.0				
		Total	Boric acid	Enrichment	FA pitch	Clad-thick
Case 1	1.00153	318 ± 51	182 ± 25	149 ± 25	207 ± 25	53 ± 25
Case 2	1.00321	359 ± 49	145 ± 25	153 ± 25	289 ± 23	31 ± 23
Case 3	1.00429	385 ± 49	148 ± 23	142 ± 23	326 ± 25	9 ± 25
Case 4	1.00483	410 ± 51	130 ± 25	154 ± 25	357 ± 25	21 ± 25
Case 5	1.00523	432 ± 45	137 ± 21	167 ± 23	374 ± 23	20 ± 21
Case 6	1.00559	468 ± 48	219 ± 23	154 ± 25	384 ± 23	2 ± 23

the verification of MCS against MCNP6. The validation studies deal with the relative comparison of pin powers calculated by MCS with the nuclear data libraries ENDF/B-VII.1 and ENDF/B-VIII.0 against the four measured maps of radial pin power.

6.1. Verification of pin-by-pin and axial power profile calculations

The comparison between MCS and MCNP6 of the radial power distribution of the 9954 pins of the VVER-1000 mock-up is first performed with the ENDF/B-VII.1 library. The fission reaction rates of the pins are tallied with the "fission" tally in MCS and the F4 tally with a FM multiplier in MCNP6. For both codes, the statistical uncertainty for a single pin equals about 0.36% (1σ) on average and reaches at the maximum 0.95% (1σ) for low-power pins. The comparison of pin-by-pin power ($C_{MCS}/C_{MCNP6} - 1$) between MCS and MCNP6 is displayed in Fig. 9. An excellent agreement is observed between the two codes, with a root-mean-square (RMS) of ($C_{MCS}/C_{MCNP} - 1$) differences equal to 0.4% ± 1.1% (3σ), a minimum difference equal to −2.3% ± 2.5% (3σ) and a maximum difference equal to 2.1% ± 1.7% (3σ).

Then, the axial power profile of the VVER-1000 mock-up calculated by MCS and MCNP6 with the ENDF/B-VII.1 library is presented in Fig. 10. The fission reaction rates are calculated with a mesh tally made of 25 axial meshes of 5 cm height each, thus covering the active fuel. The axial power profile for the VVER-1000 mock-up calculated by the diffusion code MOBY-DICK/BUGLE-96 [4] is also plotted in Fig. 10 for comparison. The axial power profiles are normalized so that the sum of the powers of the 25 axial meshes equals unity.

An excellent agreement within 1σ is observed between the axial power profiles of MCS and MCNP6. The axial power profile is not symmetric due to the insertion of six cluster absorber rods. The effect of the spacer grid modelling can be seen on the axial power profile calculated by MCS and MCNP6, with dips in power at the spacer grid locations (~25 cm, ~50 cm, ~75 cm, ~100 cm). The axial power dips are not observed in the MOBY-DICK calculation because it does not model the spacer grids.

6.2. Validation of pin-by-pin calculations

The statistical analysis of the (C/E−1) pin power discrepancies is performed with a chi-square-test. For each measured map, it is checked whether the distribution of (C/E−1) discrepancies is normally distributed with a mean value of zero and standard deviations equal to the uncertainties of the (C/E−1) values. The corresponding mathematical expression of the chi-square indicator χ^2 is given in Eq. (1) as follows:

$$\chi^2 = \sum_i \frac{\left[\left(\frac{C}{E} - 1\right)_i - \overline{X}\right]^2}{\sigma_i^2}, \quad (1)$$

where $\overline{X}$ represents the mean value of the (C/E−1) discrepancies and is assumed to be zero, and σ is the total uncertainty (experiment and calculation) at 1σ of the (C/E−1) value. A two-sided chi-square test is performed with a lower tail at 0.025 (χ^2_{low}) and the upper tail at 0.975 (χ^2_{up}), for a confidence level of $\alpha = 95\%$, and a number of degrees of freedom equal to the number of measured pins. If the indicator is between the lower and upper tail ($\chi^2_{low} < \chi^2 < \chi^2_{up}$), a statistically good agreement is observed between calculated and experimental pin powers, with a confidence level of 95%. If the indicator is smaller than the lower tail ($\chi^2 < \chi^2_{low}$), the agreement between calculated and experimental pin powers is so perfect that it is statistically "too good to be true". Finally, an indicator greater than the upper tail ($\chi^2 > \chi^2_{up}$) points towards a significant discrepancy between calculations and experiments, likely due to an underestimation of the total uncertainties and/or biases in the nuclear data.

6.2.1. MCS versus SINBAD-1

The experimental data from the SINBAD-1 benchmark (relative values of pin powers for 260 pins, normalized so that the mean value of the 260 pin powers equals 1000) is compared against MCS calculations. The pin power in the central 5-cm region of each of the 260 pins is tallied with MCS and normalized in the same way as the experimental data. The relative comparison between calculated and measured pin powers, plotted in terms of (C/E − 1) values with total uncertainties (experimental and statistical) at 3σ, is shown in Fig. 11 for the ENDF/B-VII.1 and ENDF/B-VIII.0 libraries. The x-axis represents the position of the measured pins in the assembly according to the numbering of Fig. 2. The SINBAD experimental uncertainty at 1σ for one pin ranges from 2% to 5% with RMS of 3.3%. The MCS statistical uncertainty at 1σ for one pin ranges from 0.7% to 2.6% with RMS of 1.4%. The statistical uncertainties are higher for the pins near the reactor steel baffle, in the order of 2−2.6% (1σ), due to the lower fission power close to the baffle. Individually, the pins have a C/E agreement within 3σ, except in the assembly #3 where one pin (ENDF/B-VII.1 calculation)/three pins (ENDF/B-VIII.0

Table 9
(C-E) k_{eff} discrepancies and estimated uncertainties with ENDF/B-VII.1 and ENDF/B-VIII.0

Case	C-E ± 3σ (pcm) ENDF/B-VII.1	Uncertainties 3σ (pcm)		C-E ± 3σ (pcm) ENDF/B-VIII.0	Uncertainties 3σ (pcm)	
		Tech.	Stat.		Tech.	Stat.
Case 1	137 ± 300.6	300	18	153 ± 318.6	318	18
Case 2	307 ± 370.6	370	18	321 ± 359.6	359	18
Case 3	403 ± 376.6	376	18	429 ± 385.6	385	18
Case 4	462 ± 410.4	410	15	483 ± 410.6	410	18
Case 5	495 ± 416.6	416	18	523 ± 432.4	432	15
Case 6	532 ± 451.6	451	18	559 ± 468.6	468	18

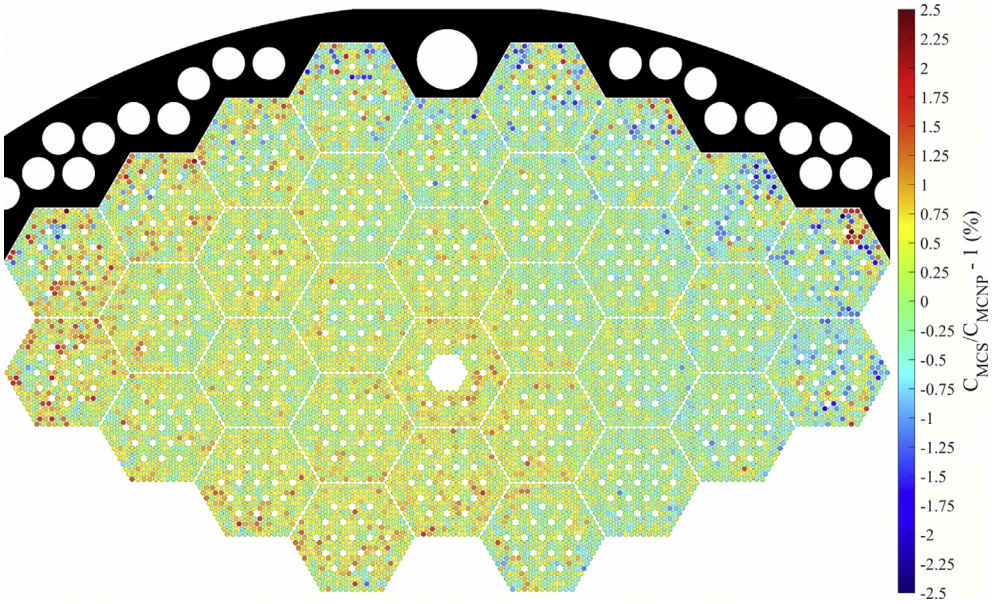

Fig. 9. Comparison ($C_{MCS}/C_{MCNP} - 1$) of pin-by-pin powers between MCS and MCNP6.

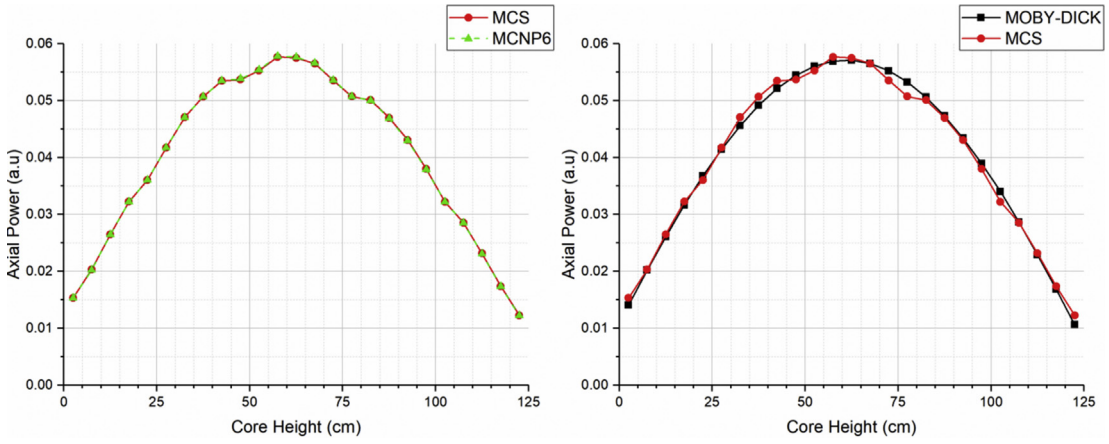

Fig. 10. Comparison of relative axial power between MCS, MCNP6 and MOBY-DICK, calculation.

calculation) underestimate the measurements outside 3σ. The minimum, maximum and RMS of the (C/E−1) values are given in Table 10. For both libraries, roughly 40% of the 260 (C/E−1) values lie outside one standard deviation and 6% outside two standard deviations. No significant differences are observed between ENDF/B-VII.1 and ENDF/B-VIII.0 for the pin power calculations.

The distribution of (C/E − 1) values for each pin of the VVER-1000 mock-up is also plotted in Fig. 12. A trend can be observed where the calculated powers underestimate the measurements close to the reactor baffle and overestimate the measurements further away from the baffle. This trend is confirmed by the chi-square test in Table 15: the chi-square test fails as the χ^2 indicators are greater than the upper tail values χ^2_{up} for both the ENDF/B-VII.1 and ENDF/B-VIII.0 libraries.

6.2.2. *MCS versus BENCHMARK-2*

The relative comparison of 52 pin powers calculated by MCS and measured during the BENCHMARK-2 experiment is conducted in this subsection. The powers in the 2-cm central region of the 52 pins are calculated with MCS with the ENDF/B-VII.1 and ENDF/B-VIII.0 libraries. The calculated and measured pin powers are normalized separately (so that the sum of the 52 pin powers equals unity) and then compared. The (C/E − 1) discrepancies between MCS and the measured data is plotted with the associated uncertainties at 3σ in Fig. 13, where the x-axis represents the numbering of the pins shown in Fig. 4. The uncertainties include the adjusted experimental uncertainties (ranging at 1σ from 1.4% to 10.4% with RMS of about 5.7%) and the statistical uncertainties from MCS (ranging at 1σ from 1.0% to 3.9% with a RMS of 2.4%). A C/E agreement within 3 standard deviations is observed individually for the 52 pins for both libraries.

The (C/E−1) discrepancies for the 52 pins are listed in Table 11. The “pin number” represents the numbering sequence of the 52 pins while the “pin position” represents the location of a pin with regards to the assembly numbering (cf. Fig. 1) and the pin numbering inside the assembly (cf. Fig. 2). No significant differences are observed between the libraries ENDF/B-VII.1 and ENDF/B-VIII.0 for the pin power calculations, with a (C/E−1) RMS value of 3.8% ± 6.1% (1σ) for ENDF/B-VII.1 and 4.8% ± 6.1% (1σ) for ENDF/B-VIII.0.

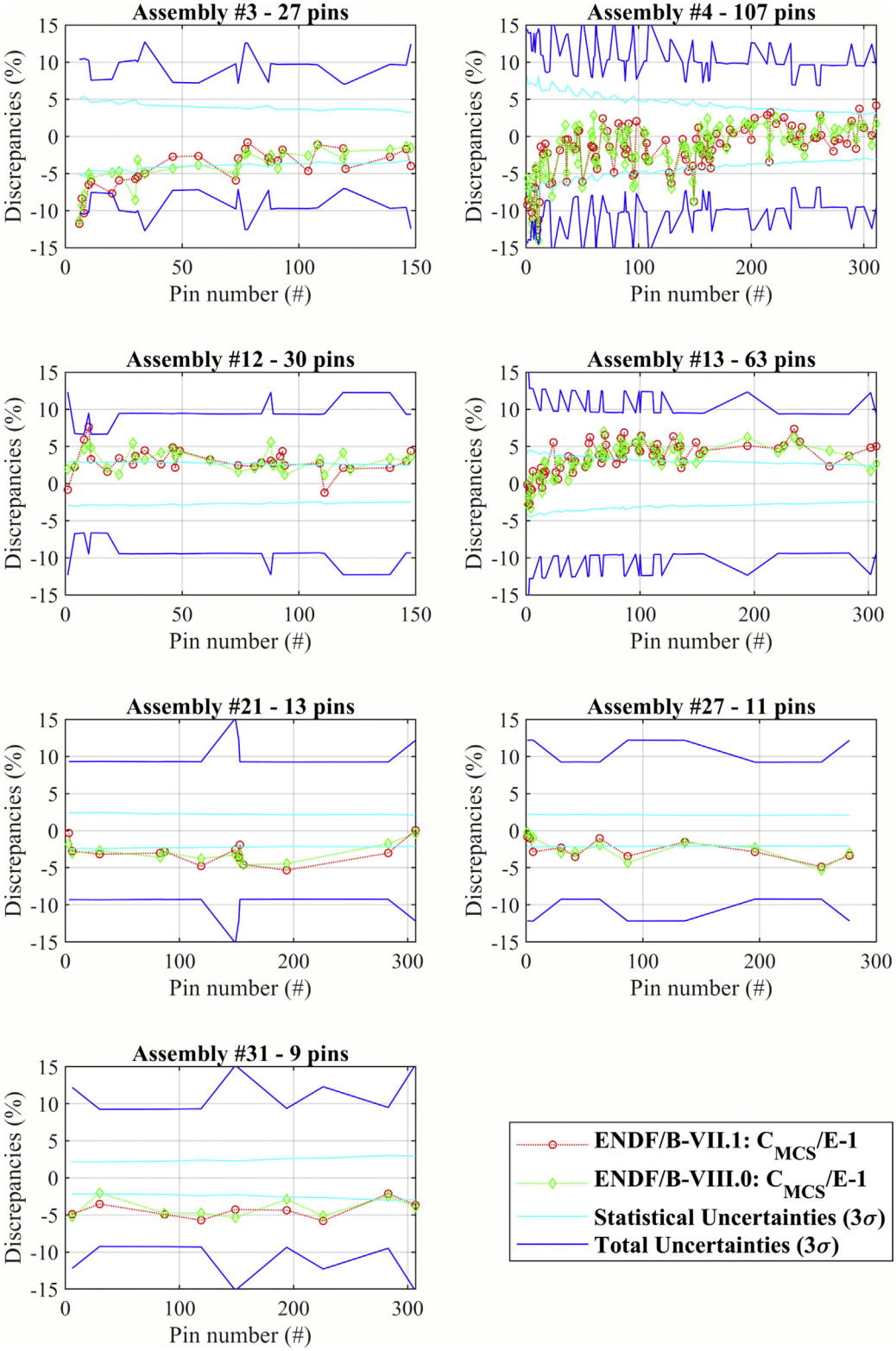

Fig. 11. Assembly-wise distribution of (C/E − 1) values for the 260 pin powers measured in the SINBAD-1 experiment.

The statistical behavior of the (C/E−1) values is analyzed with the chi-square test. The χ^2 indicators for both libraries are greater than the lower tail value χ^2_{low} and smaller than the upper tail value χ^2_{up}, as can be seen in Table 15. The chi-square tests are thus passed and show evidence of a good agreement between calculations and experiments, with (C/E−1) discrepancies that are only of statistical nature.

6.2.3. *MCS versus BENCHMARK-3*

The relative comparison of calculated and measured pin power

Table 10
Global parameters related with the discrepeancies between calculation and experiment of SINBAD-1.

Parameter	(C/E−1) ± 3σ ENDF/B-VII.1	Position of the pin	(C/E−1) ± 3σ ENDF/B-VIII.0	Position of the pin
Min	−12.6% ± 14.1%	4_10	−14.0% ± 14.5%	4_11
Max	7.6% ± 9.4%	12_10	7.0% ± 9.6%	13_68
RMS	4.1% ± 10.7%		4.0% ± 10.7%	

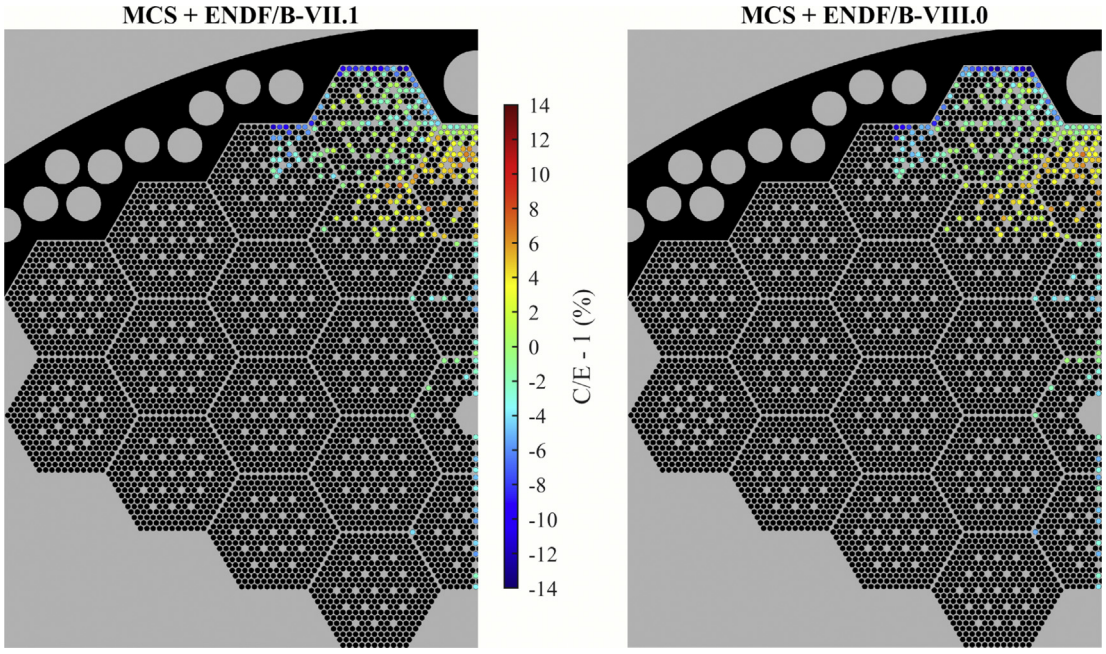

Fig. 12. Distribution of (C/E − 1) values for the 260 pin powers measured in the SINBAD-1 experiment.

Table 11
List of (C/E − 1) values for the BENCHMARK-2 experiment with ENDF/B-VII.1 and ENDF/B-VIII.0

Pin No.	Pin Pos.	B-VII.1	B-VIII.0	3σ	Pin No.	Pin Pos.	B-VII.1	B-VIII.0	3σ
1	3_149	−5.7%	−2.8%	16.6%	**27**	13_2	−4.3%	−6.8%	15.7%
2	3_1	8.2%	6.6%	15.0%	**28**	13_3	−7.1%	−8.7%	16.7%
3	3_2	2.1%	−1.4%	26.7%	**29**	13_4	−7.6%	−11.1%	16.0%
4	3_3	4.5%	−1.0%	23.9%	**30**	13_5	−1.8%	−7.4%	16.4%
5	3_4	7.5%	12.1%	26.2%	**31**	13_6	−2.8%	−5.7%	16.2%
6	3_5	3.9%	2.6%	23.2%	**32**	3_302	3.1%	7.4%	10.7%
7	3_6	−3.9%	−2.8%	21.8%	**33**	3_312	0.2%	2.9%	9.3%
8	3_7	1.3%	−3.0%	21.7%	**34**	12_149	2.8%	2.8%	9.0%
9	3_8	−4.1%	−2.0%	22.1%	**35**	3_164	−1.0%	2.8%	11.2%
10	3_9	1.3%	1.2%	21.3%	**36**	4_302	4.2%	1.6%	11.2%
11	3_10	−4.5%	1.7%	20.7%	**37**	4_312	2.5%	4.9%	9.9%
12	3_11	7.6%	4.9%	20.6%	**38**	13_149	1.7%	3.3%	9.8%
13	4_149	−2.2%	−4.9%	17.4%	**39**	12_302	−1.6%	−1.5%	7.2%
14	4_1	5.0%	11.2%	18.1%	**40**	12_312	3.2%	3.7%	7.4%
15	4_2	2.5%	0.3%	33.1%	**41**	21_149	−4.1%	−2.8%	6.3%
16	4_3	2.6%	5.2%	28.1%	**42**	12_164	0.1%	1.2%	7.9%
17	4_4	−5.7%	−4.8%	24.6%	**43**	13_302	2.2%	3.2%	7.9%
18	4_5	−2.1%	−1.7%	29.0%	**44**	21_302	4.1%	2.6%	5.1%
19	4_6	−1.6%	−6.9%	25.9%	**45**	27_149	−4.4%	−4.1%	5.9%
20	4_7	−4.8%	3.3%	28.7%	**46**	27_302	−1.8%	−3.6%	6.0%
21	4_8	1.3%	−0.7%	28.0%	**47**	31_302	−0.8%	−3.4%	9.5%
22	4_9	2.9%	4.6%	15.7%	**48**	31_303	2.6%	−1.0%	9.4%
23	4_10	0.9%	7.4%	31.1%	**49**	31_304	2.2%	1.3%	9.5%
24	4_11	−4.2%	−5.1%	32.1%	**50**	31_305	−2.1%	−1.7%	9.4%
25	4_164	−2.9%	3.5%	16.0%	**51**	31_306	0.1%	−0.6%	9.4%
26	13_1	−4.1%	−6.1%	15.1%	**52**	31_307	2.6%	0.8%	9.4%
ENDF/B-VII.1*		Max	8.2% ± 15.0%		**ENDF/B-VIII.0***		Max	12.1% ± 26.2%	
		Min	−7.6% ± 16.0%				Min	−11.1% ± 16.0%	
		RMS	3.8% ± 18.4%				RMS	4.8% ± 18.4%	

* All uncertainty values are at 3σ.

Table 12
List of (C/E − 1) values for the BENCHMARK-3 experiment with ENDF/B-VII.1 and ENDF/B-VIII.0

Pin No.	Pin Pos.	B-VII.1	B-VIII.0	3σ	Pin No.	Pin Pos.	B-VII.1	B-VIII.0	3σ
1	1_302	0.3%	0.6%	6.9%	**49**	2_8	−5.2%	−2.4%	8.0%
2	1_290	1.6%	3.3%	7.1%	**50**	2_9	−4.7%	−3.5%	8.0%
3	1_277	3.9%	−1.4%	7.3%	**51**	2_10	−6.3%	−5.2%	7.7%
4	1_263	2.0%	6.1%	7.2%	**52**	2_11	−4.9%	−3.6%	7.2%
5	1_251	1.2%	−0.1%	7.8%	**53**	3_149	−7.7%	−5.4%	7.7%
6	1_235	−2.3%	−3.7%	7.9%	**54**	3_129	−4.6%	−3.5%	7.8%
7	1_218	−0.3%	2.1%	8.1%	**55**	3_110	−3.5%	−1.8%	8.0%
8	1_119	0.7%	−1.8%	8.4%	**56**	3_96	−3.7%	−3.3%	8.0%
9	1_185	−2.4%	−2.5%	8.5%	**57**	3_79	−4.7%	−4.5%	8.2%
10	1_165	−1.3%	−5.4%	9.2%	**58**	3_63	0.1%	−2.2%	8.0%
11	1_149	3.1%	−1.0%	10.4%	**59**	3_51	2.0%	0.5%	8.5%
12	1_129	−3.0%	−2.5%	10.3%	**60**	3_37	3.3%	−1.7%	8.5%
13	1_110	−1.5%	2.1%	10.5%	**61**	3_24	−3.2%	−2.0%	8.9%
14	1_96	−3.6%	1.3%	10.6%	**62**	3_12	1.9%	−3.0%	8.7%
15	1_79	−5.6%	−1.9%	10.1%	**63**	3_1	−8.4%	−3.4%	9.8%
16	1_63	−7.8%	0.9%	10.2%	**64**	3_2	−3.2%	−3.3%	10.0%
17	1_51	−3.6%	−6.2%	10.1%	**65**	3_3	−2.0%	−6.1%	8.9%
18	1_37	−2.8%	−5.3%	10.4%	**66**	3_4	−4.8%	−1.8%	9.0%
19	1_24	−0.6%	−3.2%	10.5%	**67**	3_5	−6.0%	−2.6%	9.2%
20	1_12	−2.2%	−2.7%	10.5%	**68**	3_6	−5.5%	−5.1%	8.5%
21	1_1	−8.6%	−9.0%	11.4%	**69**	3_7	−6.5%	−7.5%	8.1%
22	1_2	−6.9%	−3.7%	10.9%	**70**	3_8	−5.3%	−2.8%	8.2%
23	1_3	−6.4%	−3.4%	10.0%	**71**	3_9	−4.8%	−6.2%	7.8%
24	1_4	−4.8%	−7.2%	9.6%	**72**	3_10	0.6%	2.1%	7.9%
25	1_5	−4.6%	−2.6%	9.5%	**73**	3_11	3.3%	3.8%	7.7%
26	1_6	−2.3%	−2.3%	9.2%	**74**	2_30	−1.9%	0.0%	7.8%
27	1_7	−9.0%	−8.4%	9.0%	**75**	2_87	2.3%	0.9%	7.4%
28	1_8	−7.5%	−6.8%	8.5%	**76**	2_119	−2.0%	−2.3%	6.7%
29	1_9	−7.7%	−8.1%	8.8%	**77**	2_194	1.4%	1.9%	7.1%
30	1_10	−8.4%	−6.1%	8.1%	**78**	2_226	2.1%	1.7%	6.5%
31	1_11	−7.2%	−7.7%	7.8%	**79**	2_283	3.5%	0.7%	6.4%
32	2_149	−2.4%	−3.2%	7.5%	**80**	2_307	0.8%	0.8%	6.3%
33	2_129	4.7%	2.6%	8.0%	**81**	10_6	3.7%	2.8%	6.3%
34	2_110	3.1%	3.8%	8.2%	**82**	10_30	3.5%	2.9%	6.3%
35	2_96	−1.8%	−2.0%	8.2%	**83**	10_87	2.6%	3.8%	5.6%
36	2_79	6.7%	2.9%	8.6%	**84**	10_119	1.9%	2.2%	6.2%
37	2_63	6.7%	4.0%	8.7%	**85**	10_194	1.4%	1.5%	5.6%
38	2_51	5.7%	2.6%	8.8%	**86**	10_226	2.7%	1.6%	5.6%
39	2_37	−2.6%	1.1%	8.6%	**87**	10_283	4.8%	4.0%	6.2%
40	2_24	−0.2%	0.4%	8.6%	**88**	10_307	4.7%	4.9%	6.1%
41	2_12	1.0%	0.0%	9.1%	**89**	18_6	3.2%	2.6%	5.6%
42	2_1	−6.2%	−6.4%	9.3%	**90**	18_30	0.4%	−1.0%	6.2%
43	2_2	−1.0%	0.0%	9.1%	**91**	18_87	−2.4%	−2.4%	6.2%
44	2_3	−3.1%	−2.4%	9.3%	**92**	18_119	2.7%	1.4%	6.3%
45	2_4	1.4%	−0.6%	8.8%	**93**	18_194	0.1%	−1.7%	6.9%
46	2_5	−1.6%	0.7%	8.8%	**94**	18_226	1.5%	3.2%	6.8%
47	2_6	−4.5%	−1.2%	8.3%	**95**	18_283	−0.1%	2.3%	7.1%
48	2_7	−5.5%	−1.2%	8.1%	**96**	18_307	−3.4%	−0.4%	7.0%
ENDF/B-VII.1*		Max		6.7% ± 8.7%	**ENDF/B-VIII.0***		Max		6.1% ± 7.2%
		Min		−9.0% ± 9.0%			Min		−9.0% ± 11.4%
		RMS		4.2% ± 8.3%			RMS		3.7% ± 8.3%

* All uncertainty values are at 3σ.

for the 96 pins of the BENCHMARK-3 experiment is presented in this subsection. The pin power in the 5-cm central region of the fuel pins is tallied with MCS and the ENDF/B-VII.1 and ENDF/B-VIII.0 libraries. The measurements and calculation are normalized separately (so that the sum of the power of the 96 pins equals unity) and are then compared.

The relative comparison between MCS calculations and measurements is shown in Fig. 14 in terms of (C/E − 1) values with their uncertainties at 3σ. The uncertainties are the quadratic sum of the adjusted experimental uncertainties (ranging from 1.7% to 2.7% with RMS of 1.7% at 1σ) and of the MCS statistical uncertainties (ranging from 0.8% to 2.7% with RMS of 1.8% at 1σ). The pins 1 to 73 have higher statistical uncertainties than the pins 74 to 96 because they are located at the rim of the mock-up core where fission power is lower. The black vertical lines on Fig. 14 represent the green-colored pins on the pin numbering shown in Fig. 5. Among the 96 measured pins, individual C/E disagreements beyond 3σ are observed for 3 pins in the ENDF/B-VII.1 calculation but are not observed in the ENDF/B-VIII.0 calculation. The full list of the (C/E−1) discrepancies is given in Table 12.

The statistical behavior of the (C/E−1) values is analyzed with the chi-square test. The χ^2 indicators for both libraries are much greater than the upper tail value χ^2_{up} as can be seen in Table 15. The chi-square is thus failed for this benchmark and is evidence of a strong statistical disagreement between calculation and experiment. However, the χ^2 indicators are notably different between the two libraries, with the χ^2 indicator for the ENDF/B-VIII.0 calculation being smaller and closer to the upper tail value than for the ENDF/B-VII.1 calculation.

Table 13
(C/E − 1) values of BENCHMARK-4 experiment for ENDF/B-VII.1 and ENDF/B-VIII.0

Pin No.	Pin Pos.	Ba-140		Ru-103		I-131		Ce-141		Zr-95	
		B-VII.1	B-VIII.0	B-VII.1	B-VIII.0	B-VII.1	B-VIII.0	B-VII.1	B-VIII.0	B-VII.1	B-VIII.0
1	2_149	−2.6%	−3.3%	−1.9%	−2.6%	−2.4%	−3.1%	−1.2%	−2.0%	−2.6%	−3.3%
2	2_129	0.7%	−1.4%	0.7%	−1.3%	0.1%	−1.9%	−2.5%	−4.5%	0.4%	−1.6%
3	2_110	1.0%	1.8%	0.2%	0.9%	1.2%	1.9%	−0.2%	0.6%	0.4%	1.1%
4	2_96	−1.8%	−2.0%	−2.6%	−2.7%	−2.5%	−2.7%	−4.3%	−4.5%	−2.3%	−2.4%
5	2_79	4.0%	0.4%	3.0%	−0.6%	3.3%	−0.4%	1.1%	−2.5%	3.7%	0.0%
6	2_63	3.2%	0.7%	2.2%	−0.3%	2.4%	−0.1%	1.3%	−1.2%	3.1%	0.5%
7	2_51	2.4%	−0.6%	1.9%	−1.1%	1.7%	−1.3%	0.0%	−2.9%	2.0%	−1.0%
8	2_37	−6.2%	−2.7%	−6.7%	−3.2%	−6.9%	−3.4%	−8.1%	−4.6%	−6.6%	−3.1%
9	2_24	−1.7%	−1.0%	−3.0%	−2.4%	−1.5%	−0.9%	−1.6%	−1.0%	−2.9%	−2.3%
10	2_12	−1.0%	−2.0%	−0.8%	−1.8%	−0.6%	−1.6%	1.1%	0.1%	−1.0%	−1.9%
11	2_1	−0.8%	−1.0%	−2.2%	−2.3%	−1.4%	−1.5%	−2.1%	−2.3%	−2.2%	−2.4%
12	2_2	2.0%	3.1%	0.2%	1.3%	0.9%	2.0%	1.3%	2.3%	−0.2%	0.9%
13	2_3	0.5%	1.2%	0.6%	1.4%	0.7%	1.5%	1.2%	1.9%	−0.3%	0.4%
14	2_4	4.4%	2.4%	4.5%	2.5%	4.7%	2.7%	5.0%	3.1%	5.6%	3.6%
15	2_5	2.6%	5.1%	1.8%	4.3%	2.5%	4.9%	2.2%	4.6%	1.4%	3.8%
16	2_6	−0.1%	3.4%	−0.1%	3.4%	0.6%	4.1%	1.4%	5.0%	−1.2%	2.3%
17	2_7	−3.5%	0.9%	−3.9%	0.5%	−2.7%	1.7%	−3.5%	0.9%	−4.1%	0.3%
18	2_8	−1.0%	2.0%	−2.3%	0.6%	−1.7%	1.3%	0.3%	3.3%	−2.6%	0.3%
19	2_9	−0.1%	1.1%	−0.3%	0.9%	0.8%	2.1%	3.3%	4.6%	−0.9%	0.4%
20	2_10	−3.1%	−2.0%	−3.5%	−2.4%	−3.7%	−2.5%	−1.6%	−0.4%	−4.0%	−2.9%
21	2_11	0.5%	2.0%	0.7%	2.2%	0.4%	1.9%	1.5%	3.0%	−0.8%	0.7%
22	2_30	−6.2%	−4.3%	−4.7%	−2.8%	−2.8%	−0.9%	−2.3%	−0.3%	−4.1%	−2.2%
23	2_87	−2.3%	−3.7%	−1.0%	−2.4%	1.2%	−0.2%	−1.4%	−2.8%	−0.3%	−1.7%
24	2_119	−1.2%	−1.5%	−0.1%	−0.4%	−3.7%	−3.9%	−1.1%	−1.3%	−1.0%	−1.2%
25	2_194	1.5%	2.0%	1.3%	1.9%	2.5%	3.1%	0.9%	1.5%	1.2%	1.7%
26	2_226	2.8%	2.4%	3.2%	2.7%	2.3%	1.9%	1.5%	1.1%	2.7%	2.3%
27	2_283	0.8%	−1.9%	2.3%	−0.4%	2.3%	−0.4%	3.0%	0.3%	2.9%	0.2%
28	2_307	1.1%	1.1%	0.1%	0.1%	−1.4%	−1.4%	−0.7%	−0.8%	1.2%	1.2%

Table 14
Global (C/E−1) parameters with uncertainties at 3σ for each fission product and the libraries ENDF/B-VII.1 and ENDF/B-VIII.0 of BENCHMARK-3 experiment.

Parameter	Library	Ba-140	Ru-103	I-131	Ce-141	Zr-95
Max	**ENDF/B-VII.1**	4.4% ± 7.0%	4.5% ± 7.9%	4.7% ± 7.0%	5.0% ± 7.6%	5.6% ± 7.6%
Min		−6.2% ± 7.2%	−6.7% ± 7.8%	−6.9% ± 7.2%	−8.1% ± 7.8%	−6.6% ± 7.8%
RMS		2.7% ± 6.8%	2.6% ± 7.5%	2.5% ± 7.0%	2.6% ± 7.7%	2.7% ± 7.4%
Max	**ENDF/B-VIII.0**	5.1% ± 6.9%	4.3% ± 7.9%	4.9% ± 6.9%	5.0% ± 7.8%	3.8% ± 7.5%
Min		−4.3% ± 7.2%	−3.2% ± 7.8%	−3.9% ± 6.6%	−4.6% ± 7.8%	−3.3% ± 6.8%
RMS		2.3% ± 6.8%	2.1% ± 7.5%	2.3% ± 6.9%	2.7% ± 7.7%	2.0% ± 7.3%

Table 15
Summary of chi-square test for pin power measurements.

Experiment name	**Measured fission product**	χ^2		**DOF**	χ^2_{low}	χ^2_{up}	**Pass/ Fail**
		ENDF/B-VII.1	ENDF/B-VIII.0				
SINBAD-1	Unknown	354.17	322.31	260	217.23	306.56	Fail
BENCHMARK-2	La-140	39.49	53.13	52	33.97	73.81	Pass
BENCHMARK-3	Sr-92	218.85	168.26	96	70.78	125.00	Fail
BENCHMARK-4	Ba-140	38.10	30.14	28	15.31	44.46	Pass
	Ru-131	29.41	18.80				Pass
	I-131	34.43	28.83				Pass
	Ce-141	29.14	33.02				Pass
	Zr-95	34.66	18.20				Pass

6.2.4. MCS versus BENCHMARK-4

The relative comparison of calculated and measured pin power for the 28 pins (5 fission products measured by pin) of the BENCHMARK-4 experiment is presented in this subsection. The fission power in the 5-cm central region of the 28 pins is tallied with MCS. The calculations and measurements are then normalized (so that the sum of the powers of the 28 pins equals unity) and compared. The (C/E−1) discrepancies are plotted in Fig. 15 with their uncertainties at 3σ. The uncertainties correspond to the quadratic sum of the adjusted experimental uncertainties (ranging from 1.2% to 2.8% with RMS of about 1.7% at 1σ) and the MCS statistical uncertainties (ranging from 1.0% to 2.2% with RMS of 1.7% at 1σ). For each pin in Fig. 15, the plotted uncertainty is the maximum value of total uncertainty between the 5 fission product measurements. The black vertical lines on Fig. 15 represent the green-colored pins on the pin numbering shown in Fig. 6.

Calculation/experiment agreement within 3σ is observed individually for the 28 pins and all the fission product measurements, for both the ENDF/B-VII.1 and ENDF/B-VIII.0 libraries. Table 13 lists all the (C/E − 1) values for each pin and each fission product. Only

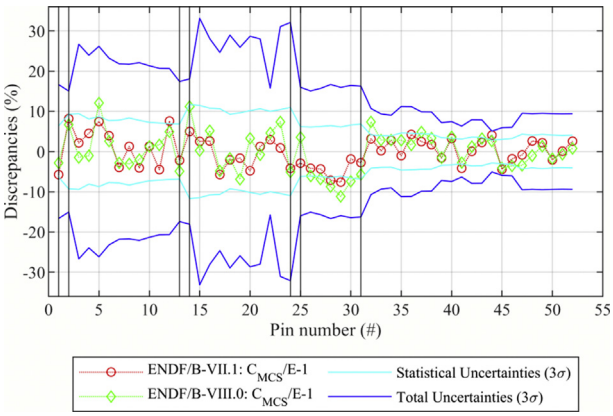

Fig. 13. Comparison of MCS pin power calculations with ENDF/B-VII.1 and ENDF/B-VIII.0 libraries versus BENCHMARK-2 experimental data.

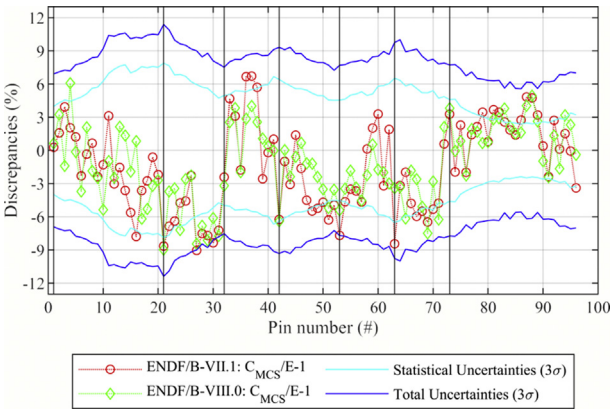

Fig. 14. Comparison of MCS pin power calculations with ENDF/B-VII.1 and ENDF/B-VIII.0 libraries versus BENCHMARK-3 experimental data.

one pin for the calculation with ENDF/B-VII.1 has a C/E disagreement outside the 3σ region for the ^{141}Ce fission product. Contrary to the other benchmarks, an underestimation trend of the calculation is not strongly observed for the pins 1 to 22 close to the reactor baffle. The maximum, minimum and RMS value of the discrepancies (C/E − 1) are listed in Table 14 for both the ENDF/B-VII.1 and ENDF/B-VIII.0 cases. The χ^2 indicators for the ENDF/B-VIII.0 calculation for the fission products ^{131}Ru and ^{95}Zr are smaller and closer to the lower tail value than for the ENDF/B-VII.1 calculation, showing improvement between the two libraries.

The statistical behavior of the (C/E−1) values is analyzed with the chi-square test. For each of the 5 measured fission products, the χ^2 indicators for both libraries are greater than the lower tail value χ^2_{low} and smaller than the upper tail value χ^2_{up}, as can be seen in Table 15. The chi-square tests are thus passed and show evidence of a good agreement between calculations and experiments, with (C/E−1) discrepancies that are only of statistical nature.

6.2.5. Discussion

The interpretation of the four pin power benchmarks has uncovered contradictory chi-square findings, which is surprising because the measurements were all performed on the same research reactor (the VVER-1000 mock-up) and the interpretation of the four benchmarks was consistently performed with the same Monte Carlo code, the same ACE nuclear data files and the same reactor model.

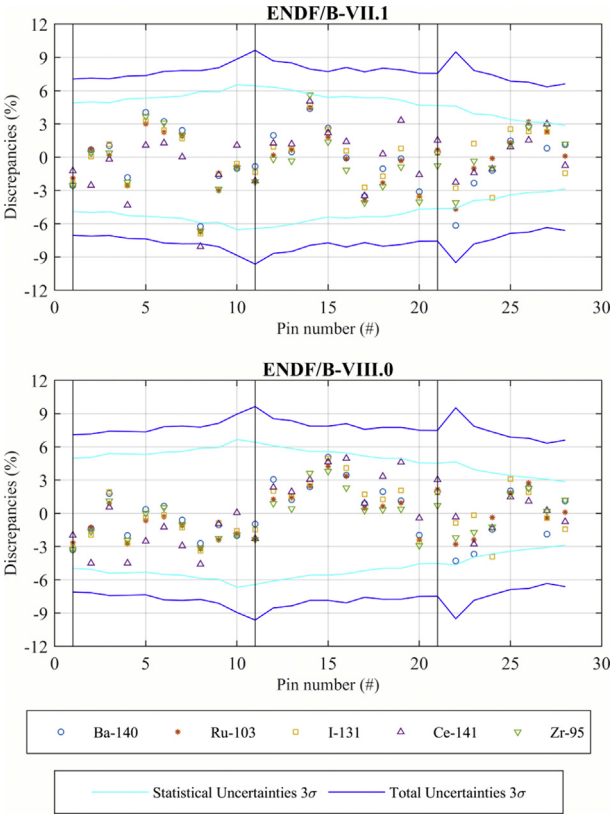

Fig. 15. Comparison of MCS pin power calculations with ENDF/B-VII.1 and ENDF/B-VIII.0 libraries versus BENCHMARK-4 experimental data.

Several possibilities to explain the contradictory chi-square findings are explored. If the measurements were performed indeed on the same research reactor, they were not performed at the same time, they were not performed with the same measurement techniques and they have been documented very unequally. Especially, the experimental conditions and the measurement techniques of the SINBAD-1 experiment (chi-square test failed) are not as well documented as the other three experiments. The components of the experimental uncertainties are also not addressed, and the experimental uncertainties may therefore have been underestimated. It is worth noticing that BENCHMARK-2 (chi-square test passed), a later experiment where relative pin powers were also measured, presents much larger experimental uncertainties than SINBAD-1, especially for the pins close to the core baffle.

The BENCHMARK-3 and BENCHMARK-4 experiments provides adequate information about the experimental setup to measure the absolute pin powers and describe satisfactorily the components of the experimental uncertainties. The interpretation of those two experiments gave opposite outcomes: the chi-square test failed for BENCHMARK-3 but passed for BENCHMARK-4. For further investigation, another C/E analysis is conducted for the 28 pins of assembly #2 that were measured in both benchmarks. The (C/E−1) values for the measurements with the fission product ^{140}Ba (BENCHMARK-4) are compared against the (C/E−1) values for the measurements with the fission product ^{92}Sr (BENCHMARK-3). This comparison is performed with the ENDF/B-VIII.0 nuclear data library, the calculations are normalized to 28 pins instead of 96 pins for the ^{92}Sr measurements, and the results are shown in Fig. 16. For the same 28 pins and the same MCS calculation normalized in the same way, the C/E agreement looks visually better for the experimental data from BENCHMARK-4 than from BENCHMARK-3.

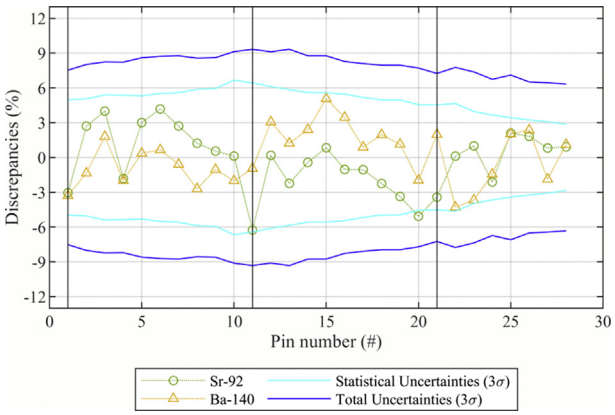

Fig. 16. Comparison between calculation and experiment for 28 pins using ^{92}Sr (BENCHMARK-3) and ^{140}Ba (BENCHMARK-4) on ENDF/B-VIII.0 library.

Globally observed, the pin power calculations for the pins close to reactor baffle (the pins facing the reactor baffle) seem to underestimate the measurements and the magnitude of the underestimation seems to be even larger for the pins located at the corner of assemblies. This effect is most visible for SINBAD-1 (cf. Fig. 12) and BENCHMARK-3 (cf. Fig. 14). This observation suggests that the powers of the pins close to the reactor baffle may be very sensitive to the size of the water gap between the outer pins and the reactor baffle, and/or that the size of this water gap may be not uniform along the reactor baffle. The analysis of the sensitivity of the pin powers to the size of the water gap is therefore performed to investigate this point.

For an assembly and fuel pin pitch of 23.6 cm and 1.275 cm respectively, the water gap between the most outer pins (measured from the outer surface of the cladding) and the reactor baffle is modelled as 3 mm long in MCS model. A perturbation of +0.5 mm to this value is implemented for the sensitivity analysis. The (C/E−1) results with uncertainties are plotted in Fig. 17 for the BENCHMARK-3 experiment, Fig. 18 for the BENCHMARK-4 experiment and the results of the chi-square test for the +0.5 mm perturbation are shown in Table 16. The results show that the +0.5 mm perturbation on the size of water gap greatly improves the pin power C/E agreement for SINBAD-1 and BENCHMARK-3 (strong decrease of the chi-square indicator). When testing the effect of the +0.5 mm perturbation for BENCHMARK-4, all the chi-square tests pass except for one (ENDF/B-VII.1 calculation for ^{140}Ba measurements) where the chi-square indicator (=45.47) is very close to the passing criterion (upper tail value of 44.46). More precise data on the size of the water gap between the outer pins and the reactor baffles may therefore be key to resolve the C/E disagreement observed for SINBAD-1 and BENCHMARK-3 during this interpretation.

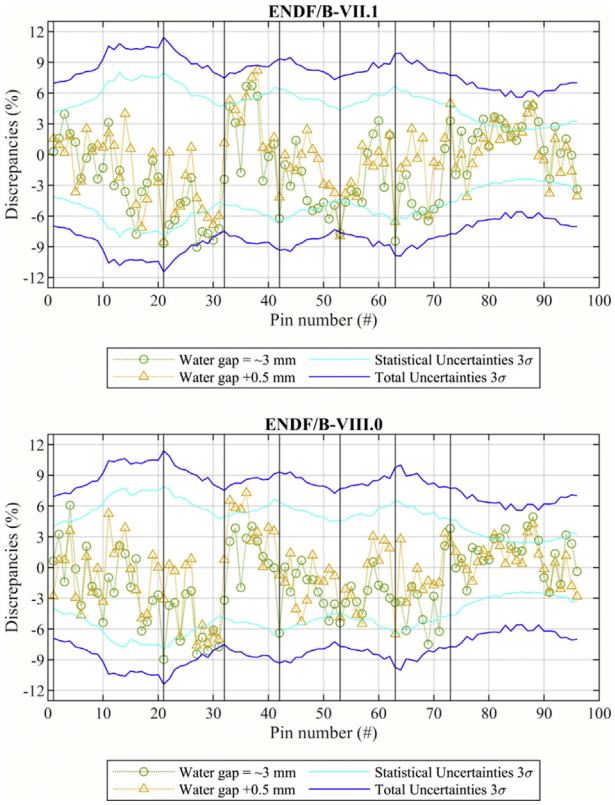

Fig. 17. Sensitivity analysis on the size of water gap for the BENCHMARK-3 experiment with ENDF/B-VII.1 and ENDF/B-VIII.0 libraries.

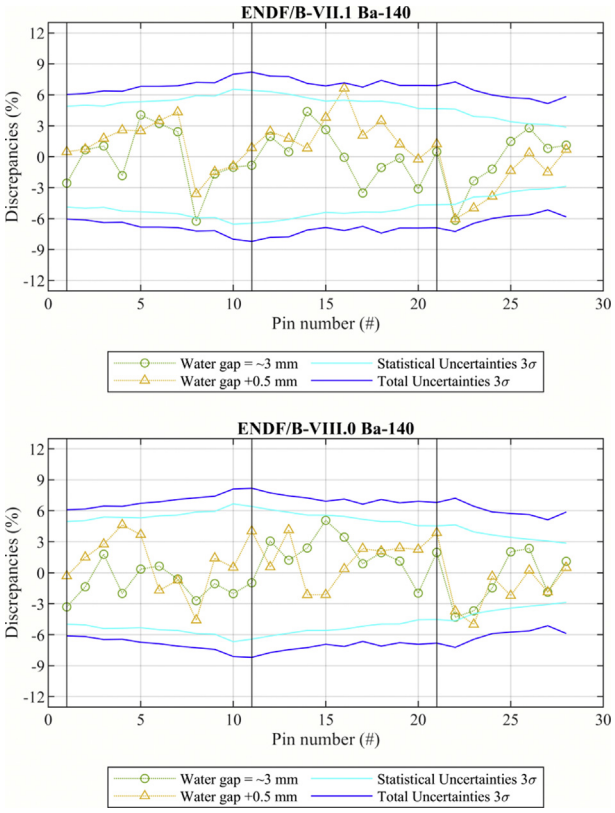

Fig. 18. Sensitivity analysis on the size of water gap for the BENCHMARK-4 experiment (^{140}Ba) with ENDF/B-VII.1 and ENDF/B-VIII.0 libraries.

7. Conclusions and perspectives

The interpretation of criticality experiments from the VVER-1000 mock-up in the LR-0 research reactor is presented to provide validation elements of the MCS + ENDF/B-VII.1 and MCS + ENDF/B-VIII.0 calculation routes applied to hexagonal-lattice light-water reactors. The investigated experimental data includes the measurements of multiplication factors for six different critical configurations and four distinct measurements of relative and absolute pin powers presented in the literature. No significant impact on the k_{eff} between the calculation with ENDF/B-VII.1 and ENDF/BVIII.0 libraries is observed despite the update of

Table 16
Summary of Chi-square test between reference and perturbated calculation of the sensitivity analysis on the water gap.

Library	Experiment name	Measured fission product	χ^2 Reference	χ^2 Perturbated (+0.5 mm)	Outcomes (Reference to Perturbated)
ENDF/B-VII.1	SINBAD-1	Unknown	354.17	250.19	Fail to Pass
	BENCHMARK-3	Sr-92	218.85	147.19	Fail to Fail
	BENCHMARK-4	Ba-140	38.10	45.47	Pass to Fail
		Ru-131	29.41	26.26	Pass to Pass
		I-131	34.43	38.03	Pass to Pass
		Ce-141	29.14	37.01	Pass to Pass
		Zr-95	34.66	25.60	Pass to Pass
ENDF/B-VIII.0	SINBAD-1	Unknown	322.31	255.53	Fail to Pass
	BENCHMARK-3	Sr-92	168.26	132.53	Fail to Fail
	BENCHMARK-4	Ba-140	30.14	39.36	Pass to Pass
		Ru-131	18.80	25.26	Pass to Pass
		I-131	28.83	32.40	Pass to Pass
		Ce-141	33.02	37.59	Pass to Pass
		Zr-95	18.20	21.61	Pass to Pass

important nuclides. For the pin power analysis, using the ENDF/B-VIII.0 library decreases significantly the chi-square indicators in some cases but also increases them slightly in other cases.

The analysis of the six critical configurations shows a consistent overestimation of the k_{eff} values, with k_{eff} (C-E) values ranging from +137 to +532 pcm. The average k_{eff} (C-E) value equals +389 pcm for ENDF/B-VIII.0 and + 411 pcm for ENDF/B-VII.1. The sensitivity of the k_{eff} to four technological parameters of the mock-up (boric acid concentration, fuel enrichment, fuel assembly pitch, cladding thickness) is performed and the evaluated technological uncertainty for the six critical configurations ranges from 300 pcm to 468 pcm at three standard deviations. More efforts should be conducted in the future to quantify other sources of uncertainty such as the impact of the modelling of the spacer grids and the uncertainty due to nuclear data (with a sensitivity analysis of the k_{eff} to the nuclear data and the propagation of the nuclear data covariance matrices).

The validation studies on pin power are done by means of relative comparison between MCS and four distinct pin power measurement campaigns. An underestimation trend is observed for the pins facing the reactor baffle for SINBAD-1 and BENCHMARK-3, leading to a statistically significant C/E disagreement. A sensitivity analysis of the pin powers to the size of the water gap between outer pins and reactor baffle shows that a perturbation of +0.5 mm on a gap of 3 mm greatly improves the C/E agreement for those two benchmarks, and more precise information is therefore needed on the size of the water gap for further analysis. Conversely, a good and statistically significant C/E agreement is observed for the BENCHMARK-4 interpretation, even for the pins close to the reactor baffle, and this C/E agreement remains nearly unchanged even with a perturbation of +0.5 mm on the water gap. Of the four studied pin-power benchmarks, BENCHMARK-4 benefitted from the experimental feedback of the other three benchmarks, it is the most documented benchmark and it presents the lowest experimental uncertainties.

This interpretation represents a first step towards the shielding analysis of the VVER-1000 mock-up (analysis of the shielding measurements detailed in SINBAD-1 benchmark), as accurate calculations of the pin power distribution in the core, especially for pins close to the baffle, are required before calculating the resulting neutron and gamma photon flux in the external components of the core. The shielding analysis will provide validation elements to the neutron-photon transport capability and variance reduction techniques of the MCS Monte Carlo code when applied to the calculation of the neutron fluence in the external components of VVER cores. Furthermore, this work will provide a reference solution for the verification of the two-step STREAM/RAST-K code developed inhouse at UNIST for the criticality analysis of hexagonal fuel lattice.

Declaration of competing interest

The authors declare that they have no known competing financial interests or personal relationships that could have appeared to influence the work reported in this paper.

Acknowledgements

This work was supported by the National Research Foundation of Korea (NRF) grant funded by the Korea government (MSIT). (No. NRF-2019M2D2A1A03058371).

Appendix A. Supplementary data

Supplementary data to this article can be found online at https://doi.org/10.1016/j.net.2020.06.015.

References

[1] K. Ilieva, S. Belousov, A. Ballesteros, et al., Reactor dosimetry for VVERs RPV lifetime assessment, Prog. Nucl. Energy 51 (2009) 1–13.
[2] M. Košťál, M. Schulc, V. Rypar, et al., VVER-1000 Mock-Up Physics Experiments Hexagonal Lattices (1.275 Cm Pitch) of Low Enriched U(2.0, 3.0, 3.3 wt.% 235U)O2 Fuel Assemblies in Light Water with H3BO3, OECD/NEA IRPhE Project, LR(0)-VVER-RESR-002, 2006.
[3] M. Koštál, V. Rypar, V. Jurícek, The criticality of VVER-1000 mock-up with different H3BO3 concentration, Ann. Nucl. Energy 60 (1) (2013) 1–7.
[4] B. Osmera, J. Mikus, F. Hudec, et al., Radiation Field Parameters for Pressure Vessel Monitoring in VVER-1000 Using the NRI LR-0 Experimental Reactor (~1990), OECD/NEA SINBAD REACTOR, 2009. Package NEA-1517/82.
[5] M. Košťál, V. Rypar, M. Švadlenková, The pin power distribution in theVVER-1000 mock-up on the LR-0 research reactor, Nucl. Eng. Des. 242 (1) (2012) 201–214.
[6] M. Košťál, M. Švadlenková, J. Milčák, Absolute determination of power density in the VVER-1000 mock-up on the LR-0 research reactor, Appl. Radiat. Isot. 78 (1) (2013) 38–45.
[7] M. Košťál, M. Švadlenková, J. Milčák, et al., Determination of critical assembly absolute power using post-irradiation activation measurement of week-lived fission products, Appl. Radiat. Isot. 89 (1) (2014) 18–24.
[8] B. Ebiwonjumi, S. Choi, M. Lemaire, et al., Verification and validation of radiation source term capabilities in STREAM, Ann. Nucl. Energy 124 (2019) 80–87.
[9] J. Choe, S. Choi, P. Zhang, et al., Verification and validation of STREAM/RAST-K for PWR analysis, Nucl. Eng. Technol. 51 (2) (2019) 356–368.
[10] H. Lee, W. Kim, P. Zhang, et al., "Mcs – a Monte Carlo particle transport code for large-scale power reactor analysis," Ann. Nucl. Energy, vol. 139, 2020.
[11] V. Dos, H. Lee, Y. Jo, et al., Overcoming the challenges of monte-carlo depletion: application to a material-testing reactor with MCS code, Nucl. Eng. Technol. 52 (9) (2020) 1881–1895.
[12] J. Jang, W. Kim, S. Jeong, et al., Validation of UNIST Monte Carlo code MCS for criticality safety analysis of PWR spent fuel pool and storage cask, Ann. Nucl. Energy 114 (2018) 495–509.

[13] J. Yu, H. Lee, M. Lemaire, H. Kim, et al., MCS based neutronics/thermal-hydraulics/fuel-performance coupling with CTF and FRAPCON, Comput. Phys. Commun. 238 (2019) 1–18.
[14] T.Q. Tran, J. Choe, X. Du, et al., Preliminary CEFR analysis by Monte Carlo codes, in: M&C 2019, Oregon, USA, 2019.
[15] M. Chadwick, M. Herman, P. Oblozinsky, et al., ENDF/B-VII.1 nuclear data for science and Technology: cross sections, covariances, fission product yields and decay data, Nucl. Data Sheets 112 (2011), 2887-2996.
[16] D.A. Brown, M.B. Chadwick, R. Capote, et al., ENDF/B-VIII.0: the 8th major release of the nuclear reaction data library with CIELO-project cross sections, new standards and thermal scattering data, Nucl. Data Sheets 148 (2018) 1–142.
[17] X.B. Tran, N.Z. Cho, A study of neutronics effects of the spacer grids in a typical PWR via Monte Carlo calculation, Nucl. Eng. Technol. 48 (1) (2016) 33–42.
[18] M. Nowak, J. Miao, E. Dumonteil, et al., Monte Carlo power iteration: entropy and spatial correlations, Ann. Nucl. Energy 94 (2016) 856–868.